Marine Geology 403 (2018) 1–19

Contents lists available at ScienceDirect

Marine Geology

journal homepage: www.elsevier.com/locate/margo

Insights into barrier-island stability derived from transgressive/regressive state changes of Parramore Island, Virginia

Jessica L. Raff[a,*,1], Justin L. Shawler[b], Daniel J. Ciarletta[c], Emily A. Hein[b], Jorge Lorenzo-Trueba[c], Christopher J. Hein[b]

[a] Department of Geology, College of William & Mary, P.O. Box 8795, Williamsburg, VA 23187-8795, USA
[b] Virginia Institute of Marine Science, College of William & Mary, P.O. Box 1346, Gloucester Point, VA 23062-1346, USA
[c] Department of Earth and Environmental Studies, Montclair State University, 1 Normal Ave, Montclair, NJ 07043, USA

ARTICLE INFO

Editor: E. Anthony

Keywords:
Barrier island
Progradation
Antecedent geology
Foredune ridge
Beach ridge
Inlet

ABSTRACT

Barrier islands and their associated backbarrier ecosystems front much of the U.S. Atlantic and Gulf coasts, yet threshold conditions associated with their relative stability (i.e., state changes between progradation, erosion, and landward migration) in the face of sea-level rise remain poorly understood. The barrier islands along Virginia's Eastern Shore are among the largest undeveloped barrier systems in the U.S., providing an ideal natural laboratory to explore the sensitivity of barrier islands to environmental change. Details about the developmental history of Parramore Island, one of the longest (12 km) and widest (1.0–1.9 km) of these islands, provide insight into the timescales and processes of barrier-island formation and evolution along this mixed-energy coast. Synthesis of new stratigraphic (vibra-, auger, and direct-push cores), geospatial (historical maps, aerial imagery, t-sheets, LiDAR), and chronologic (optically stimulated luminescence, radiocarbon) analyses reveals that Parramore has alternated between periods of landward migration/erosion and seaward progradation during the past several thousand years. New chronology from backbarrier and barrier-island facies reveals that Parramore Island has existed in some form for nearly 5000 years. Following a period of rapid overwash-driven retrogradation, and coinciding with a period of slow relative sea-level rise (~1 mm/ yr), Parramore stabilized ~1000 years ago in partial response to pinning by and sediment delivery from erosion of a Pleistocene-aged antecedent high. Following pinning, Parramore built seaward through development of successive progradational beach and dune ridges. Morphological and historical evidence suggests that these processes were interrupted by inlet formation—possibly associated with an interval of enhanced storminess—at least three times during this period. Following inlet closure in the early 1800s, island progradation was rapid, with Parramore Island reaching its maximum width ca. 150 years ago. It has since switched states again, undergoing accelerating erosion (~12 m/ yr since 1980). The relative youth of Parramore Island is in contrast to many East Coast barrier islands, which generally reached their present positions about 3500–2000 years ago. Moreover, these results demonstrate that the apparent robustness and stability of Parramore are ephemeral features of an island that has undergone multiple state changes within the last 1000 years. Finally, they refine current knowledge of the roles of antecedent topography, sediment delivery rates, storms, and sea-level rise in barrier-island stability and resilience to future climate change.

1. Introduction

Barrier islands front approximately 5000 km of the U.S. Atlantic and Gulf coasts (Davis and FitzGerald, 2004), with the 405 islands within this region comprising 24% of the total global barrier-island shoreline length (Stutz and Pilkey, 2011). Globally, barrier islands, and their backbarrier marshes and tidal flats, provide key ecosystem services (Barbier et al., 2011), protect mainland coasts from large storm events (Otvos, 2012), and are hosts to economically important communities and infrastructure (Brander et al., 2006). Barrier islands are typically composed of a shoreface and barrier platform, beach and adjacent foredune, beach and dune ridges, inlets and tidal deltas, lagoon, marsh, and mainland coast (Oertel et al., 1992; Davis and FitzGerald, 2004); these components are together referred to as a "barrier system".

* Corresponding author.
E-mail addresses: jessica.l.raff@vanderbilt.edu (J.L. Raff), jshawler@vims.edu (J.L. Shawler), ciarlettad1@mail.montclair.edu (D.J. Ciarletta), eahein@vims.edu (E.A. Hein), lorenzotruej@mail.montclair.edu (J. Lorenzo-Trueba), hein@vims.edu (C.J. Hein).
[1] Present Address: Department of Earth and Environmental Sciences, Vanderbilt University, PMB 351805, 2301 Vanderbilt Place, Nashville, TN 37235-1805, USA.

https://doi.org/10.1016/j.margeo.2018.04.007
Received 12 January 2018; Received in revised form 12 April 2018; Accepted 15 April 2018
Available online 19 April 2018
0025-3227/ © 2018 Elsevier B.V. All rights reserved.

In response to the high degree of dynamism observed along barrier islands, including undergoing sub-decadal periods of erosion, growth, migration, and rotation, recent studies have attempted to approach these systems holistically—from the shoreface to the backbarrier marshes and lagoons—to fully understand the mechanisms responsible for observed changes (e.g., Brenner et al., 2015; Deaton et al., 2017; Lorenzo-Trueba and Mariotti, 2017). Over millennial time scales, the effects of climate change and relative sea-level rise (RSLR) are the dominant cause of landward barrier-island migration (Wolinsky and Murray, 2009; Moore et al., 2010; Brenner et al., 2015). Several additional factors play significant roles in the rate of shoreline retreat and barrier-island migration by influencing the balance between accommodation creation (generally due to RSLR) and infilling (due to net sediment inputs). Among these are increased storminess and human development (e.g., Rogers et al., 2015); antecedent topography and inland slope (e.g., Wolinsky and Murray, 2009; Lorenzo-Trueba and Ashton, 2014; Ashton and Lorenzo-Trueba, 2018); and substrate erodibility, slope, and sediment fluxes (e.g., Moore et al., 2010). Walters et al. (2014) and Brenner et al. (2015) together demonstrate the roles that underlying substrate, barrier width, backbarrier deposition rates, and the presence/absence of marsh can have on barrier-island migration rates with respect to RSLR. They establish that backbarrier deposition, which fills newly developed accommodation space, is crucial to maintaining a subaerial barrier island. Similarly, Lorenzo-Trueba and Mariotti (2017) show that an essential component of barrier-island resilience to RSLR is a steady supply of fine sediment to the backbarrier from overwash processes. Similar barrier-backbarrier couplings form the foundation of the "runaway transgression" model (FitzGerald et al., 2008, 2018), which suggests that a reduction in sediment supply (or an increased rate of RSLR) can cause the drowning of backbarrier marshes and lead to an increase in backbarrier tidal prism and inlet ebb-tidal-delta volumes and attendant erosion and thinning of adjacent barrier islands. In this conceptual model, increased frequency of overwash of beach/shoreface sediment to the backbarrier drives the collapse of barrier-island dunes, leading to eventual breaching and inundation as the island narrows, and fostering accelerated landward migration.

Despite the new insights into the interactions between barrier islands and backbarrier environments that have emerged from conceptual and numerical models, field investigations treating these as coupled systems have been rare. Furthermore, the threshold rates of RSLR, storminess, and cross- and long-shore sediment delivery rates required for barrier-island state changes between transgressive/destructive and regressive/constructive phases remain unknown.

This study investigates the forces responsible for morphologic and sedimentologic change along the Virginia Barrier Islands (VBI) through an examination of the formation and evolutionary history of centrally located Parramore Island. Specifically, it focuses on past barrier-backbarrier system couplings for Parramore Island and how they are preserved in the present topography and stratigraphy. Analysis of the history of change along Parramore Island serves to place the evolution of the VBI alongside regional relative sea-level (RSL) changes. Furthermore, the exploration of morphologic transitions of Parramore Island over the past 1000–2000 years provides insight into the processes responsible for the formation of mixed-energy and progradational barrier islands, with implications for the stability of other barrier-island systems and associated infrastructure and natural resources.

2. Regional setting

2.1. Coastal and physical setting

Parramore Island is approximately 12 km long and 2 km wide and is located within The Nature Conservancy's Virginia Coast Reserve, along the southern Delmarva coast (Fig. 1a). Parramore is characterized by complex shore-normal to shore-parallel dune ridges to the north and a series of semi-shore-parallel dune ridges and swales in the north-central part of the island. These ridges include the ~3 km long, > 7 m high, 60–120 m wide "Italian Ridge", the highest feature along the VBI (McBride et al., 2015). Along the southern 8 km of the island, there are a series of low, segmented ridges and swales (including larger, named features such as Little Beach, South Little Beach, and Revels Island; see Fig. 1b, c), marsh, tidal channels, and circular, sandy, vegetated, isolated dunes (i.e., "pimples", sensu Hayden et al., 1995). The entire island is fronted by a narrow beach and shore-parallel foredune ridge.

Parramore Island fronts the mainland of the Virginia Eastern Shore, the 100 km long, 5–15 km wide, southern-most portion of the Delmarva Peninsula. This feature originally formed as a spit that prograded progressively southward (Oertel and Overman, 2004) during a series of former Pleistocene sea-level highstands, filling former lowstand channels of the Susquehanna River (Oertel and Foyle, 1995; Foyle and Oertel, 1997). These lowstand paleochannels, likely dating to 600–120 ka, today act as stabilizing locations for tidal inlets along the VBI (Krantz et al., 2016), including the 14.5 m deep Wachapreague Inlet and 18 m deep Quinby Inlet that bound Parramore Island to the north and south, respectively. Between these inlets are barrier islands composed primarily of unconsolidated sand, silt, and clay, and backed by saltmarshes (predominantly low marsh) and open-water lagoons.

Tides along the VBI are semi-diurnal with a mean tidal range of 1.23 m, and a mean spring range of 1.37 m (Fenster and McBride, 2015). The mean wave height is ~0.95 m, based on a record covering 2012 to 2015 (Fenster and McBride, 2015). Dominant winds are from the north (associated with northeast extratropical storms), leading to net southerly nearshore current and wave directions, and thus net southerly longshore sediment transport (Finkelstein and Ferland, 1987; Fenster et al., 2016).

The Virginia coast experiences both hurricanes and intense northeast storms, although the latter are recognized to be the primary agent of geomorphic change (Hayden and Hayden, 2003). Hayden (2003) documents a gradual increase in the frequency of cyclone impacts along the VBI between 1885 and 2002, with notable periods of reduced storminess in the 1940s and 1970/80s; these changes are reflected in system-wide, decadal-scale shoreline-change rates, which gradually track storm-impact frequencies (Fenster et al., 2017).

2.2. Holocene sea-level history

Initial barrier-island formation along the Virginia coast coincided with a gradual deceleration in RSLR during the middle to late Holocene (Newman and Rusnak, 1965; Finkelstein and Ferland, 1987; Van de Plassche, 1990; Engelhart et al., 2009). Available RSL curves from this region are based on widely-spaced data dominated by marine- and terrestrial-limiting points, with few index points (Engelhart and Horton, 2012). These local records indicate that RSLR along the Virginia coast slowed from a time-averaged rate of 1.6–1.7 mm/ yr to ca. 1.0 mm/ yr around 1500 years ago (Fig. 2). It has since undergone significant acceleration due to local subsidence and glacial isostatic adjustment (Boon et al., 2010), reaching approximately 5 mm/yr in the last 50 years (Boon and Mitchell, 2015). Higher-resolution curves available from North Carolina reveal that RSLR accelerated to ca. 1.3 mm/ yr between 1000 and 450 years ago in response to the Medieval Climate Anomaly, followed by a deceleration to ~1.0 mm/ yr until the end of the 19th century (Kemp et al., 2011).

2.3. Barrier-system morphology

Despite long-term exposure to similar RSL changes, tidal range, storm impacts, and overall wave climate, the VBI are highly diverse with respect to their morphologies and shoreline-change trends. The barrier chain is categorized into three morphological groups on the basis of shoreline-retreat rates and orientation (Fig. 1a): 1) a northern set of landward-migrating barrier islands retreating parallel to the mainland shore along what is often referred to as the "Arc of Erosion"

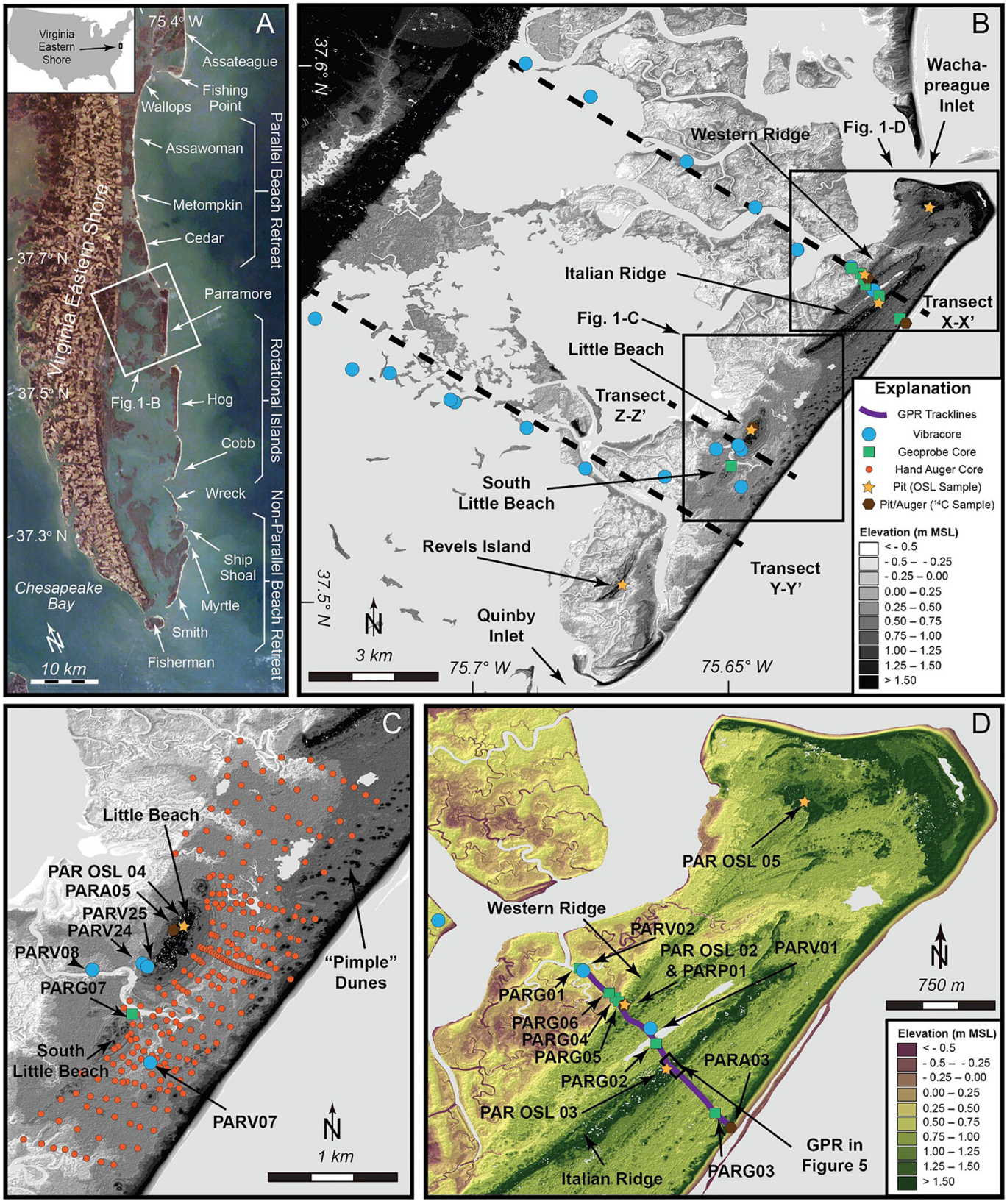

Fig. 1. Study site and field sample maps of Parramore Island on Virginia's Eastern Shore. A) Virginia's barrier islands, located along a mixed-energy reach of the Atlantic Coast, are categorized according to their shoreline behavior. To the north, a set of shore-parallel-retreat barriers are undergoing rapid shoreward migration; the central islands are experiencing rotation; and the southern islands are undergoing non-shore-parallel landward migration. B) Study site showing three primary transects of vibra- and direct-push cores. Additional samples were taken from pits and augers for optically stimulated luminescence and radiocarbon dating. C) Detailed view of the broad swale between Little Beach (a prominent topographic high on Parramore Island) and the modern beach was mapped using transects of hand auger cores. D) Detailed view of sample locations on northern Parramore Island. Note the shore-parallel ridge morphology along north-central Parramore and recurved, inlet-associated ridges on the far northern end.

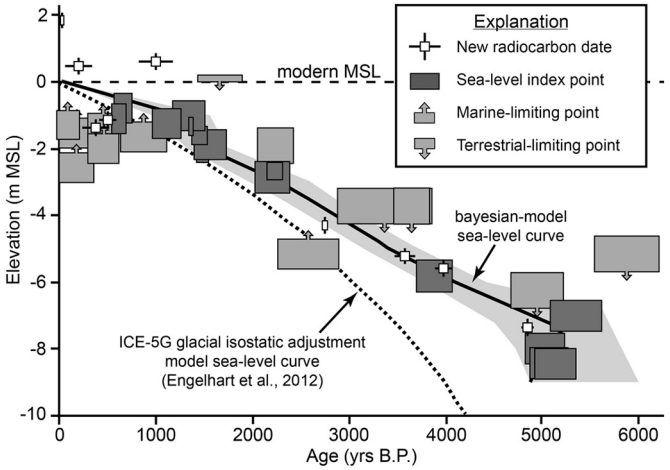

Fig. 2. Relative-sea-level curve for the Virginia Atlantic coast with new dates (Table 1) plotted for comparison. Sea-level database presented by Engelhart et al. (2009) is re-calibrated with Intcal13 and Marine13 (Reimer et al., 2013) calibration curves (see Supplemental Table 1 for details). Vertical and temporal errors (uncertainties) are given by heights and widths of data rectangles. Horizontal (age) errors represent the full range of possible calibrated ages and incorporate instrument error. The sea-level curve (solid black line) and associated error window (gray) is constructed using only sea-level index points (as identified by Engelhart et al. (2009), with 2-σ error bars) using the Clam 2.1, a R-based Bayesian age-depth modeling software (Blaauw, 2010).

(Wallops, Assawoman, Metompkin, Cedar islands), 2) a central group of largely stationary barrier islands which, due to differential erosion and accretion, have undergone apparent rotation (Parramore, Hog, Cobb islands), and 3) a southern set of barrier islands migrating and retreating sub-parallel to the mainland shore (Wreck, Ship Shoal, Smith, Myrtle islands) (Leatherman et al., 1982; Kochel et al., 1985; Fenster and McBride, 2015). The central, rotational islands (including Parramore Island, the focus of this study) display the classic drumstick morphology of mixed-energy barrier islands, characterized by numerous inlets and large ebb-tidal deltas (Hayes, 1979).

Recent work has demonstrated that ocean-shoreline change along the VBI is accelerating; time-averaged system-wide (Assawoman to Smith islands) shoreline retreat increased from 5 m/yr over the 1850–2010 period to 7 m/yr from 1980 to 2010, with individual islands experiencing varying rates or transitions between retreat and growth (Deaton et al., 2017). Shoreline change associated with barrier-island migration (landward translation), as opposed to erosion (island narrowing), has caused the net loss of nearly 63 km^2 of backbarrier marsh through burial and shoreface exposure and erosion since the 1870s (Deaton et al., 2017).

3. Methods

The middle-to-late Holocene geologic and evolutionary history of Parramore Island was investigated using a suite of field, laboratory, and geospatial methods, including sedimentological, geophysical, and geochronological analyses, as well as analysis of maps and aerial imagery.

3.1. Field data collection and mapping

Barrier-island and backbarrier stratigraphic units were characterized using a total of 19 vibracores and seven direct-push cores. Vibracores (2.5–9.0 m long) were collected along three sub-parallel transects, two of which spanned from the barrier island to the mainland (Fig. 1b). Direct-push cores (~4–12 m long), which, like vibracores, retain fine stratigraphy and sedimentary structures, were collected along one transect on northern Parramore and at the single accessible site on southern Parramore using a Geoprobe Model 66DT machine.

More than 2 km of ground-penetrating radar (GPR) data were collected across Parramore Island in one long (1700 m) cross-barrier transect and two short (200 m and 550 m) east-west transects using a MALA Geosciences X3M unit with a 500 MHz shielded antenna. Although this unit is commonly capable of imaging 2–6 m below the surface, depth penetration was commonly limited to < 1 m due to signal attenuation by high-salinity ground-water.

Five locations along subaerial ridges were targeted for optically stimulated luminescence (OSL) dating (Fig. 1). Samples for dating were collected by insertion of 30 cm opaque PVC tubes into walls of hand-dug pits from between 30 and 100 cm below the ground surface. These were retrieved, capped, and sealed under an opaque blanket cover to ensure minimal exposure of sand grains to sunlight.

Finally, the shallow stratigraphy of the interior of central Parramore Island was mapped through the collection of 260 auger cores along 25 shore-normal transects across a swale between Little Beach and the modern primary foredune ridge (Fig. 1c).

All core and sample locations and elevations were determined using a Topcon HiPer V system with real-time kinematics (RTK-GPS), providing centimeter to sub-centimeter horizontal accuracy and vertical accuracy of ~1.5 cm. Where interference from dense vegetation prevented use of the RTK-GPS, a DGPS or Garmin handheld GPS was used to obtain horizontal positions and elevations were derived from a high-resolution, LiDAR-derived topobathymetric model provided by the US Geological Survey (2016). All GPS and LiDAR data were corrected from NAVD88 to local mean sea level (MSL) through comparison with the nearby NOAA tide gauge in Wachapreague, VA.

3.2. Laboratory analysis

All sediment cores were split, photographed, described for texture (as compared to standards), mineralogy, and color (using a Munsell Soil Color Chart), and sampled for select grain-size and radiocarbon-dating analyses. Grain-size samples were analyzed using a Beckman-Coulter Laser Diffraction Particle Size Analyzer.

Ground-penetrating radar data were post-processed (site-specific filtering, migration, and variable gain control) and time-depth converted using a migration-derived radar velocity of 7 cm/ns using the RadExplorer (DECO-Geophysical Co. Ltd) software package. Topographic correction was based on LiDAR-derived elevation data.

Geochronologic control is provided by radiocarbon samples from various depths in auger holes, pits, vibracores, and direct-push cores (Table 1). Accelerator mass spectrometer radiocarbon analyses of nine shell and peat samples were performed at the National Ocean Sciences Accelerator Mass Spectrometry Facility (NOSAMS; Woods Hole, MA, USA). All radiocarbon ages were calibrated using OxCal 4.2 (Bronk Ramsey, 2009) which includes a reservoir correction. Terrestrial samples (peat roots) were calibrated with the Intcal13 calibration curve (Reimer et al., 2013). Marine samples (all mollusks) were calibrated using the Marine13 curve (Reimer et al., 2013), corrected to a ΔR of 54 ± 74 years (average of northern and southern VBI values from Rick et al. (2012)).

Additional geochronology was provided by OSL analyses of five samples at the Luminescence Dating Laboratory of the University of Georgia (Table 2). After opening samples under dark room conditions and removing 5 cm from the top and bottom (to avoid any sediment unintentionally exposed to sunlight during collection), samples were treated with 10% hydrochloric acid (HCl) and 20% hydrogen peroxide (H_2O_2) to remove carbonate and organic material. The sediment was then dried and sieved to separate grains in the ~2.7–2.0 phi size range. Quartz grains from these samples were isolated by density using liquids (densities 2.62 g cm^{-3} and 2.75 g cm^{-3}). These sediments were then treated with hydrofluoric acid (HF) before additional treatment in HCl and exposure under blue light for 1 min at 125 °C (Aitken, 1998; Bøtter-Jensen and Murray, 2001). OSL analyses were performed using a Risø TL/OSL-DA-15 Reader (Markey et al., 1997). The equivalent dose was

Table 1
Results of accelerator-mass-spectrometer radiocarbon analyses of samples collected at Parramore Island, VA. Sample IDs are given by core name: PARG – Geoprobe direct push core; PARP – hand-dug pit; PARV – vibracore; PARA – hand auger core. Sample depths are in meters relative to MSL, derived from RTK-GPS points or 2016 Chesapeake Bay Topo-bathymetric digital elevation model (USGS, 2016). ^{14}C ages were calibrated using OxCal 4.2 (Bronk Ramsey, 2009), which includes a reservoir correction. Terrestrial samples (peat roots) were calibrated with Intcal13 (Reimer et al., 2013) calibration curves and marine samples (all mollusks) were calibrated using Marine13 (Reimer et al., 2013), corrected to a ΔR of 54 ± 74 years (average of northern and southern VBI values from Rick et al., 2012).

All dates in text are reported as 2-sigma median calibrated ages before 1950 (in bold) with error derived from full range of possible calibrated ages and incorporating instrument error.

Sample ID	NOSAMS accession #	Latitude	Longitude	Elevation (m MSL)	Stratigraphic unit	Dated material	Reported age (^{14}C yrs BP)	δ^{13}C (‰ VPDB)	Cal. 2-σ age (yrs BP)	Probability (%)
PARP01: 55 cm	OS-127570	37.55886	−75.62364	0.61	V-d	*Crassostrea virginica*	1,490 ± 20	0.54	**989 ± 180**	**95.4**
PARA03: 30 cm	OS-127550	37.55163	−75.61693	1.82	V-e	Freshwater wetland peat	Modern	−25.91	**Modern**	**100.0**
PARA05: 130 cm	OS-127549	37.53090	−75.64477	0.47	V-d	Terrestrial soil	155 ± 15	−23.07	**189 ± 139** 196 ± 28 19 ± 14 269 ± 14 146 ± 9	**95.4** 48.0 19.6 15.7 12.1
PARV02: 160–164 cm	OS-127571	37.56144	−75.62622	−1.37	III	Crassostrea virginica	775 ± 15	1.18	**364 ± 139**	**95.4**
PARV02: 545–547 cm	OS-127717	37.56144	−75.62622	−5.21	III	Saltwater peat	3,330 ± 35	−16.00	**3,564 ± 106** 3,554 ± 88 3,675 ± 3	**95.4** 94.6 0.8
PARV04: 767.5–772.5 - cm	OS-134777	37.57240	−75.64386	−7.35	III	Saltwater peat	4,240 ± 20	−15.09	**4,835 ± 65** 4,837 ± 19 4,740 ± 14	**95.4** 89.0 6.4
PARV10: 445.5–450.5 - cm	OS-134778	37.531770	−75.68598	−4.29	III	Saltwater peat	2,590 ± 20	−15.56	**2,738 ± 17**	**95.4**
PARG01-D9: 56–61 cm	OS-137436	37.56150	−75.62637	−9.87	II	Paleosol (bulk sediment)	45,200 ± 6,600	−26.90	> **42,681**	**95.4**
PARG04-D2: 33–38 cm	OS-134775	37.55925	−75.62404	−1.16	V-b	Saltwater peat	410 ± 20	−14.56	**490 ± 87** 485 ± 28 344 ± 5	**95.4** 91.7 3.7
PARG04-D5: 109 cm	OS-134776	37.55925	−75.62404	−5.55	III	Saltwater peat	3,650 ± 20	−15.00	**3,964 ± 91** 3,947 ± 50 4,058 ± 21	**95.4** 76.4 19.0
PARG04-D10: 75–80 cm	OS-137334	37.55925	−75.62404	−11.17	II	*Mulinia lateralis*	26,200 ± 930	0.50	**29,915 ± 1,845**	**95.4**

determined following the single-aliquot regenerative-dose protocol set forth by Murray and Wintle (2000) using three regenerative points, a zero-dose point, and a repeat point. Twenty-four aliquots were measured and accepted if the recycling ratio was 0.9–1.1 and recuperation was ≤5%. Dose rate was calculated using the activities of uranium and thorium (measured using a thick source Daybreak alpha counting system) and potassium (measured by ICP90 using sodium peroxide fusion at the SGS Laboratory in Toronto; detection limit: 0.01%). After measurement, the uranium, thorium, and potassium contents were then converted to determine the alpha, beta, and gamma dose rates (Aitken, 1985, 1998).

Table 2
Results of optically stimulated luminescence (OSL) analyses. PAR OSL 02 did not contain enough material to acquire an OSL result.

Sample	Depth	Quartz grain	Aliquots	De	Radionuclide concentrations			Moisture	Dose rate	Age
	(m)	(μm)	Number	(Gy)	U (ppm)	Th (ppm)	K (%)	(%)	(Gy/ka)	(yrs before 2016)
PAR OSL 01 Location: 37.50188, −75.66835	0.25	150–250	24(17)	0.6 ± 0.02	0.62 ± 0.08	1.18 ± 0.33	0.95 ± 0.10	20 ± 5	1.07 ± 0.11	560 ± 60
PAR OSL 02 Location: 37.55888, −75.62365	0.57				8.03 ± 1.44	25.82 ± 8.63	0.6 ± 0.10	Insufficient sample		
PAR OSL 03 Location: 37.55487–75.62073	1.73	150–180	24(20)	0.44 ± 0.02	4.29 ± 0.47	6.44 ± 1.63	0.9 ± 0.10	10 ± 5	2.10 ± 0.20	210 ± 20
PAR OSL 04 Location: 37.53098, −75.64447	0.90	150–180	24(16)	0.19 ± 0.01	0.98 ± 0.09	1.97 ± 0.35	1.0 ± 0.10	10 ± 5	1.34 ± 0.12	140 ± 20
PARL OSL 05 Location: 37.57218, −75.61107	0.86	150–180	24(18)	0.25 ± 0.01	1.29 ± 0.25	3.72 ± 0.88	1.0 ± 0.10	20 ± 5	1.33 ± 0.13	190 ± 20

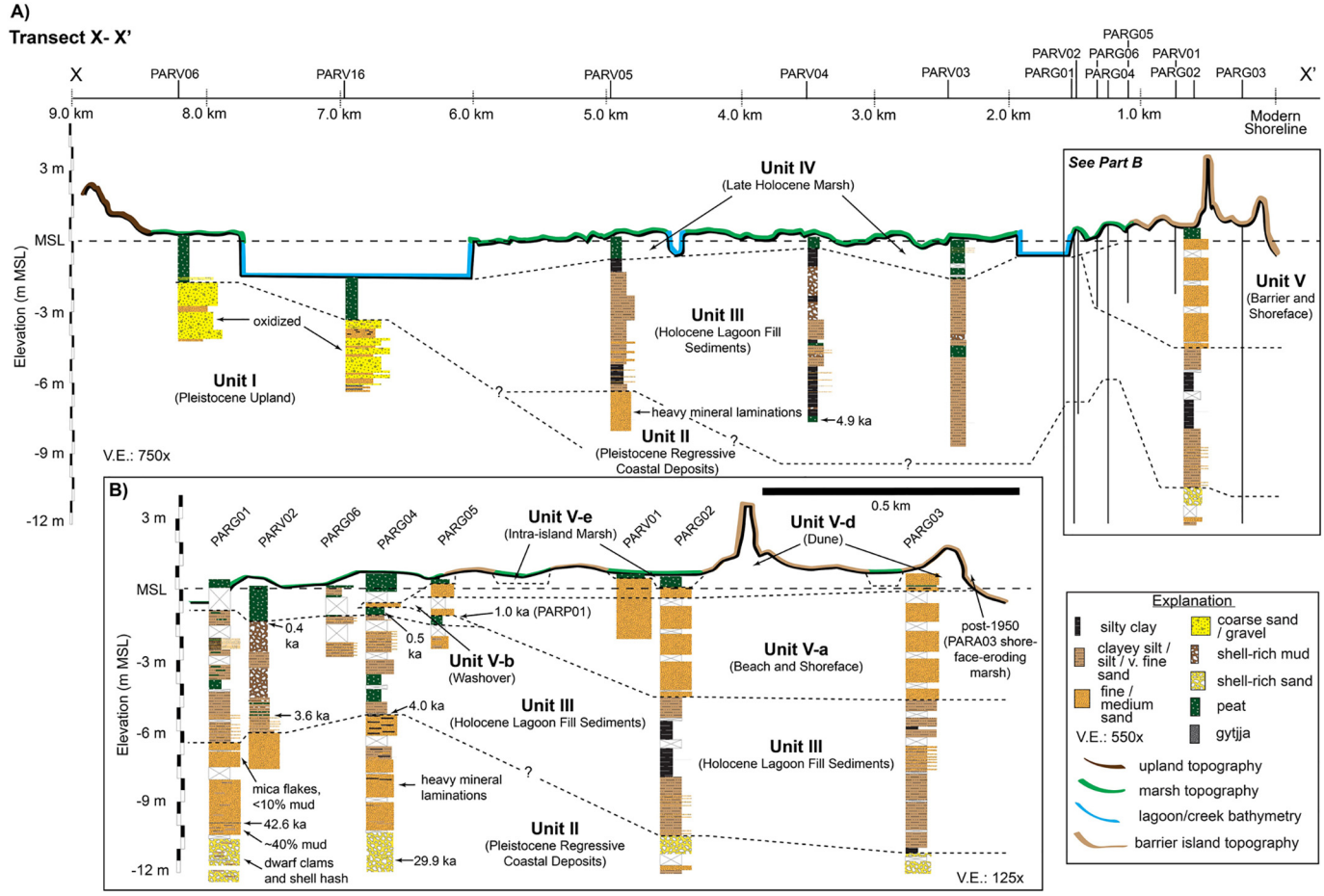

Fig. 3. Shore-perpendicular stratigraphic cross section (Transect X-X'; see location, Fig. 1b) along the northern portion of Parramore Island and its backbarrier. A) Stratigraphy derived from vibracore and Geoprobe direct-push core data from this study. Horizontal scale is in kilometers from the modern ocean-side barrier-island shoreline. The vertical scale is in meters relative to mean sea level (MSL). Core elevations are from RTK-GPS points (error: ± 1.5 cm) or LiDAR (error: ± 15–20 cm). The surface topographic profile is derived from LiDAR (USGS, 2016). Section B) provides additional detail from eastern-most, cross-barrier cores.

3.3. Geospatial analysis

A map of the sand surface underlying marsh and tidal flats in central Parramore was created through interpolation of depth-to-sand data from 260 auger cores in ArcGIS by kriging. Subaerial ridges visible in a digital elevation model developed from high-resolution LiDAR (USGS, 2016) were mapped and traced using ArcGIS. Historical maps, charts, and imagery (Carey and Lea, 1822; US Coast Survey, 1855; US Coast and Geodetic Survey, 1933; FSA, 1967) were reviewed to aid understanding of beach-ridge morphology, the chronology and extent of shoreline and morphological changes, and overall evolution of the island during the last 200 years.

4. Results

4.1. Sedimentology

Lithologic boundaries were determined from sediment cores. Sediments are divided into five stratigraphic units based on sedimentological characteristics including grain size, sorting, roundness, mineralogy, and age (Figs. 3, 4). These are described below and summarized in Table 3. Where available, a range of median grain sizes from multiple samples of the same unit/subunit is given.

4.1.1. Unit I

At the base of the backbarrier stratigraphic sequence is a heterogeneous layer of dark brown (oxidized) to gray/dark gray (10 YR 6/2 and 10 YR 4/21, respectively; Munsell, 2000), fine- to coarse-grained, subrounded to subangular quartz sand (median grain size: 2.5–1.6 phi) and gravel with minor silt and heavy mineral components. The upper contact of this unit is found at 1.5 to 3.0 m below mean sea level (m MSL) proximal to the mainland; cores in the central and eastern backbarrier did not penetrate to this unit. Increased silt and clay components characterize the uppermost 0.1 to 0.7 m of this unit, which is otherwise largely void of shells and organic matter. Heavy minerals and coarser grains are concentrated in bands of fine to medium sand adjacent to the mainland behind northern Parramore (Fig. 3), and the sediments comprising this unit exhibit slight fining-upwards adjacent to the mainland behind southern Parramore (Fig. 4).

4.1.2. Unit II

This unit is semi-compacted and composed of dark gray (10 YR 4/1) to brown (10 YR 4/3) or bluish gray (GLEY 1–5/N), subrounded to rounded, moderately well-sorted to well-sorted, fine- to medium- (median grain size: 3.1–2.8 phi) grained, quartz-dominated sand with heavy minerals. There is rare muddy sand or sandy mud (median grain size: 4.1–3.4 phi), usually with clay or silt in the form of laminations or clasts. While largely void of macro fossils, the unit contains abundant dwarf clam shells (*Mulinia lateralis*) and shell hash below 10 m MSL. Unit II is shallowest (upper contact ca. ~ −5.5 to −6.0 m MSL) below the easternmost (island-proximal) and westernmost (mainland-adjacent) portions of the backbarrier marsh/lagoon; cores in the central backbarrier did not penetrate to this unit. Deeper Geoprobe cores collected into this unit on Parramore Island proper (PARG01 and 04)

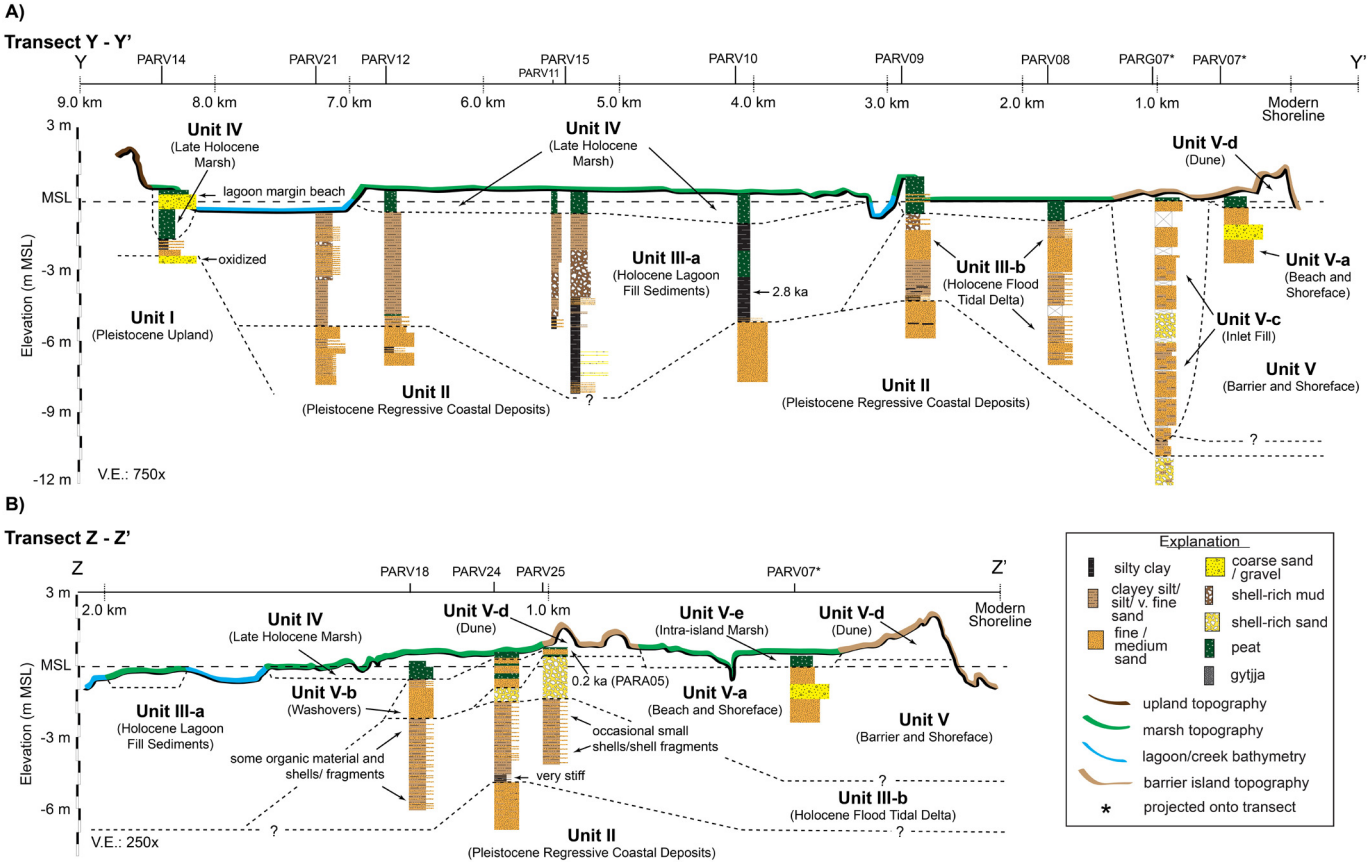

Fig. 4. Shore-perpendicular stratigraphic cross sections from southern and central Parramore Island and its backbarrier. Stratigraphy derived from vibracore and Geoprobe direct-push core data from this study. Horizontal scales are in kilometers from the modern ocean-side shoreline. The vertical scales are in meters relative to mean sea level (MSL). Core elevations are from RTK-GPS points (error: ± 1.5 cm) or LiDAR (error: ± 15–20 cm). Surface topographic profiles are derived from LiDAR (USGS, 2016). A) Transect Y-Y′ (see location, Fig. 1b). B) Transect Z-Z′ (see location Fig. 1b), a short core transect collected adjacent to, and west of, Little Beach.

reveal that it is > 5 m thick.

4.1.3. Unit III

Unit III is composed of dark gray (10 YR 4/1), spatially heterogenous silt, clay, and very fine to fine sand. The upper contact of this unit reaches to approximately −1.0 m MSL across most of the backbarrier. Unit III is thickest (> 8 m) in the central backbarrier and pinches out both landward and seaward. Because of its spatial heterogeneity, we subdivide Unit III into two subunits. Unit III-a consists of dark gray (10 YR 4/1) silt (median grain size: 6.8–6.0 phi) with occasional clay lenses, silty sand (median grain size: 3.5–3.3 phi), and sandy silt (median grain size: 5.2–3.9 phi). It commonly exhibits a gradual, slight fining upwards from silty sand to interbedded sandy silt and silt. Unit III-b consists of dark gray (10 YR 4/1) subrounded to rounded, fine to medium quartz sand (3.4–3.3 phi) with heavy minerals and minimal silt and clay; Unit III-b is found proximal to the modern barrier island.

4.1.4. Unit IV

Composed of highly organic-rich, grayish-brown (10 YR 4/2) silt and clay with some subrounded quartz sand with mica, Unit IV comprises the uppermost section of the backbarrier from approximately +1.0 to −2.2 m MSL in most locations. The sand component is dominated by medium to coarse sand with occasional granule-sized grains in mainland-proximal cores, but is absent in central backbarrier cores. The organic materials present in these sediments are largely rootlets, rhizomes, and marsh grasses (dominantly *S. alterniflora* and *S. patens*). Unit IV is thickest proximal to the mainland and barrier island, but within central Parramore Island (the mapped region shown in Fig. 6c), it is commonly < 0.5 m thick.

4.1.5. Unit V

Unit V comprises and immediately underlies the modern barrier surface. It consists primarily of fine to medium sand, with subunits of variable organic content, texture, and grain size. Subunit V-a, located at the base of this unit, is largely devoid of organic material, but contains occasional shells and shell fragments. It consists of dark gray (10 YR-4/1) subrounded fine to medium sand (median grain size: 3.3–2.4 phi) with frequent heavy mineral banding. Basal sand in Unit V-a is subrounded medium-quartz sand with heavy mineral banding. Sediment below about 1 m MSL is dominantly medium grained. A GPR profile imaging this unit in north-central Parramore (Fig. 5) reveals a 40 m long, ~1 m thick package of landward-dipping reflectors (12–13°) between about 0.75 and 1.25 m MSL, which overlies a set of high amplitude seaward-dipping reflectors (2–3°) located between approximately −0.5 to 1.0 m MSL.

Subunit V-b is found stratigraphically above and adjacent to subunit V-a. It consists of dark gray (10 YR-4/1) and light brownish gray (10 YR-6/2) fine to medium quartz sand (median 3.3–2.4 phi) with heavy minerals interbedded with dark gray (10 YR-4/1) organic-rich mud, and is found proximal the landward margin of the barrier island at depths of 0.0 to −2.5 m MSL.

Subunit V-c is found only in PARG07 (Fig. 4a) and consists of dark gray (10 YR-4/1 and 2.5 Y-5/1) muddy very fine to medium sand (median 3.3–2.5 phi) with shell hash. It is found between approximately −2.0 to −8.5 m MSL.

Subunit V-d comprises all shore-parallel ridges across Parramore, Little Beach, Revels Island, etc., as well as the surface sediments of all circular “pimple” dunes in central Parramore. Sedimentologically, this unit consists primarily of fine quartz sand with rare medium sand grains

Table 3
Description and interpretation of stratigraphic units identified within the Parramore Island barrier system.

Unit ID	Location	Depth range (m MSL)	Sedimentology	Interpretation	Age
Unit I	Mainland-proximal backbarrier	−1.5 to −3.0 m and deeper, where present	Heterogeneous, subrounded to subangular, fine to coarse quartz sand and gravel; minor silt and heavy minerals	Terrestrial upland	Pleistocene to early Holocene
Unit II	Island- and mainland-proximal backbarrier; underlying Parramore Island	−5.5 to −6.0 m and deeper, where sampled	Semi-compacted subrounded to rounded, moderately well-sorted to well-sorted, fine to medium quartz sand with heavy minerals	Pleistocene regressive coastal (beach/shoreface/dune) deposits	Pleistocene (stage 5?)
Unit III	Ubiquitous throughout backbarrier and under barrier island	−10 to −1 m	Spatially heterogenous silt, clay, and very fine/fine sand	Lagoon fill	5,500–1,000 yrs BP
Unit III-a	Throughout backbarrier (thickest segments) and underlying island	−10 to −1 m	Silt with occasional clay lenses, silty sand, and sandy silt	Lagoon-fill mud	
Unit III-b	Backbarrier proximal to barrier island and modern tidal inlets	−8 to −1 m	Subrounded to rounded, fine to medium quartz sand with heavy minerals	Paleo-flood-tidal delta	
Unit IV	Ubiquitous throughout backbarrier	−1 m to surface	Highly organic-rich silt and clay with some subrounded quartz sand with minor mica in mainland-proximal segments	Modern saltmarsh	~1,500 yrs to present
Unit V	Ubiquitous throughout barrier island	To +7 m	Fine to medium sand, with subunits of variable organic content, texture, and grain size	Barrier island complex	≤1,000 yrs BP
Unit V-a	Ubiquitous throughout barrier island		Subrounded, fine to medium sand; low organic content; occasional shells and shell fragments; some heavy minerals	Beach and shoreface	
Unit V-b	Proximal to landward margin of barrier island	−2.5 to 0 m	Interbedded fine to medium quartz sand with heavy minerals; some organic-rich mud	Washover	
Unit V-c	Landward side of central Parramore, north of South Little Beach	−8.5 to 2.0 m	Muddy very fine to medium sand with shell hash	Inlet fill	
Unit V-d	Shore-parallel, topographically high ridges; circular "pimple dunes" in central Parramore	0 to +7 m	Fine quartz sand with rare medium sand component and heavy minerals	Aeolian dunes	
Unit V-e	Between shore-parallel ridges; topographically low areas of island	−0.5 to +0.5 m	Organic-rich silt and very fine/fine sand	Inter-dune swales	

and heavy minerals. A 2 m long hand auger core (Fig. 5) from Italian Ridge reveals that the sediments composing the ridge are homogenous, primarily fine grained, well-sorted quartz-rich sand. The subsurface structure of this unit is parallel or subparallel to the surface topography, as revealed by reflections in GPR from Italian Ridge on north-central Parramore (Fig. 5). This subunit varies in depth/height with barrier island topography and ranges from +7 m MSL (Italian Ridge) to about 0 m MSL.

Subunit V-e consists of black (10 YR-2/1) to dark gray (10 YR-4/1) organic rich silt and very fine to fine sand. It is generally found between −0.5 and 0.5 m MSL. The thickness of this unit is typically < 0.5 m but auger cores reveal that it reaches thicknesses of ~1 m toward the south of the wide swale comprising central Parramore. Organic material in this unit consists of saltmarsh species common to Virginia (e.g., *Spartina patens*, *S. alterniflora*).

4.2. Geochronology

Calibrated radiocarbon ages (Table 1) range from modern (PARA03) to ^{14}C "dead" (> 42,000 yrs BP). All calibrated Holocene ^{14}C dates are plotted on an updated RSL curve for the Virginia Eastern Shore coast (Fig. 2), developed with dates re-calibrated from published records using updated radiocarbon-calibration curves (Supplemental Table 1). Although inclusion of these new dates in the RSL database is prevented due to unclear indicative meaning of most of the associated samples, we note that all four saltwater peat dates from Unit III plot within RSL error bounds.

Dates from OSL analyses (Table 2) range from 140 ± 20 years before 2016 at 0.9 m below the surface of Little Beach (PAR OSL 04) to the oldest age of 560 ± 60 years before 2016, 25 m below the western side of Western Ridge (the westernmost ridge separating Parramore Island from the backbarrier marsh; see location, Fig. 1d).

4.3. Geospatial analysis and geomorphology

Analysis of a LiDAR-derived topo-bathymetric digital elevation model (USGS, 2016) of Parramore Island (Fig. 6a) highlights spatial variations in the orientation, height, spacing, and morphology of subaerial ridges. In northern-most Parramore Island, proximal to Wachapreague Inlet, ridges have varying orientations. North-central Parramore, by contrast, is characterized by distinct ridges oriented between shore-parallel to shore-sub-parallel. Ridges northwest of Italian Ridge are spaced at 80–200 m (average: 136 m), with heights ranging from ~1.5 to 2.0 m MSL. Italian Ridge itself reaches to > 8 m MSL in some locations and is commonly > 50 m wide. The set of ridges southeast of Italian Ridge are spaced 30–130 m apart, with an average crest spacing of 82 m and heights generally < 1.5 m MSL. The primary subaerial ridges of Little Beach, South Little Beach, and Revels Island are roughly aligned with Italian Ridge. A set of smaller (~0.5 m high) ridges are observed proximal to Little Beach and Revels Island (Fig. 6a). In all cases, these smaller ridges have a distinctive curvature and are more closely spaced (~10–40 m) than the larger shore-sub-parallel ridges located on the northern part of the island.

Analyses of historical maps (Fig. 7) add context to OSL and radiocarbon chronology and to the timing and processes responsible for the development of Parramore Island. During the middle to late 18th century, the features of Parramore Island currently identified as Little Beach and Revels Island are shown as two distinct islands, separated from one another and from the area of northern Parramore Island (Carey and Lea, 1822; Fig. 7a). Coastal surveys (US Coast Survey, 1855; Fig. 7d) later depict a singular island stretching from northern Parramore south to Revels Island. The extension of Parramore south to its current position is shown in maps from the 1930s (US Coast and Geodetic Survey, 1933; Fig. 7e), whereas central and southern Parramore had undergone inundation and drowning by the 1960s (FSA, 1967; Fig. 7f).

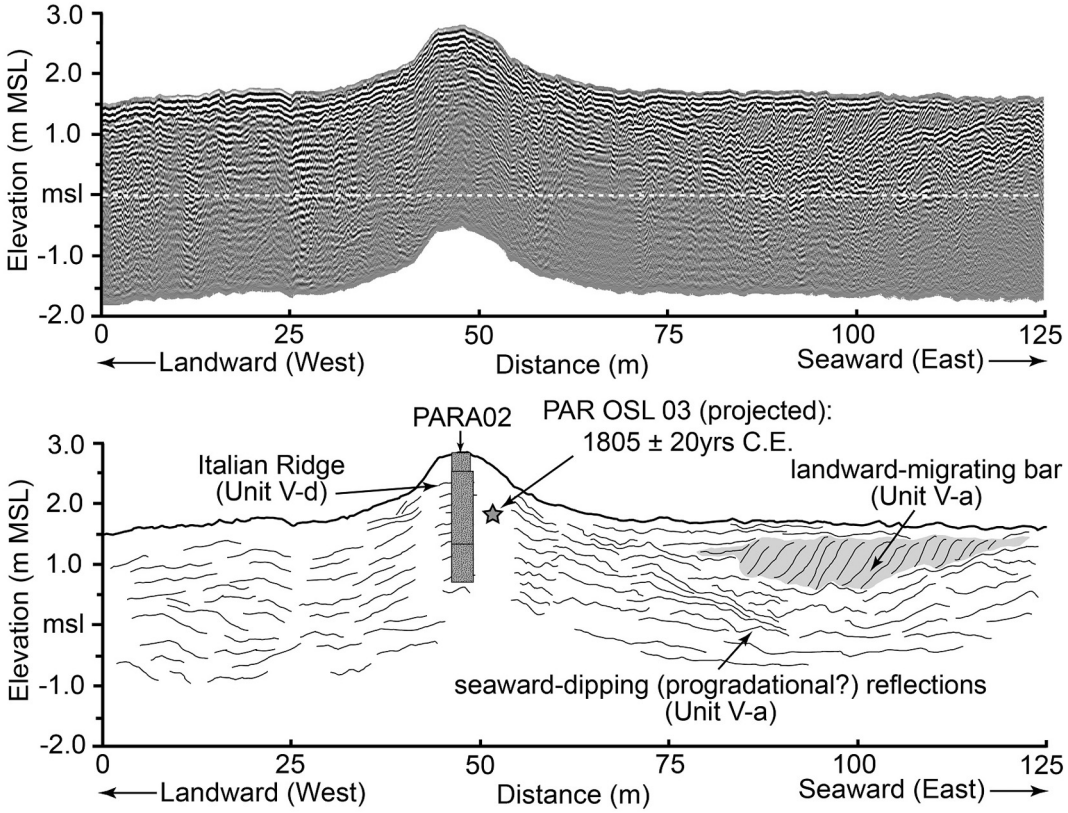

Fig. 5. Processed (top) and interpreted (bottom) ground-penetrating radar profile from across Italian Ridge on north-central Parramore Island (see location, Fig. 1d). Profile ends at the start of low-elevation swales on either side. Sediment auger core is composed entirely of fine- to medium-sized, clean, well-sorted sand with a variable heavy mineral component; the upper 35 cm contains soil-derived organic matter.

5. Discussion

5.1. Interpretation of units

5.1.1. Unit I: Pleistocene upland deposits

Unit I shares similarities in sedimentology and spatial extent to the pebble-rich, fine to coarse sand unit described by Halsey (1978) and Finkelstein and Ferland (1987). It is interpreted as upland deposits and a seaward extension of the subaerial Delmarva land surface. Both previous studies conclude that this unit is Pleistocene in age (published dated samples from this unit were often beyond the limits of ^{14}C). Halsey (1978) encounters the unit in borings from the backbarrier of Assateague Island, while Finkelstein and Ferland (1987) sample the unit proximal to the mainland in the backbarriers of Metompkin, Hog, and Smith islands (see Fig. 1a for island locations). The authors describe an additional pre-Holocene sub-unit consisting of compacted blue-green lagoonal mud; however, this sub-unit is not encountered in cores from this study.

5.1.2. Unit II: Pleistocene coastal deposits

Unit II correlates to a gray fine to very fine sand first described by Finkelstein and Ferland (1987) as a basal Holocene sand flat formed by concentration of sand at the bottom of a wide, open lagoon by locally generated waves. However, Oertel et al. (1989) demonstrate using stratigraphic relationships, sedimentologic analyses, and pollen assemblages (dominated by boreal pollen) from a southern extension of these deposits behind Cobb Island, that this unit is pre-Holocene in age. Two new radiocarbon dates confirm the Pleistocene age of this unit: a paleosol sample from core PARG01 has a calibrated age of > 42,000 years BP, while a dwarf clam (*Mulinia lateralis*) shell from PARG04 returns a calibrated age of 29,915 ± 1845 years BP. The age discrepancy is most likely due to recrystallization of younger carbon within the calcium carbonate shell. Given the burial depth of this unit (reaching to within 5.5 m of modern MSL), as well as its sedimentological maturity and degree of compaction, it is interpreted as regressive beach or dune deposits, likely associated with a Marine Isotope Stage 5 sea-level highstand. These deposits are inconsistently observed along the landward margin of Parramore Island backbarrier marshes and lagoons, where they unconformably overlie coarser upland deposits. The upper contact of this surface dips seaward, below the depth of core penetration, across the central backbarrier. However, it is observed again proximal to, and underlying, Parramore Island. In total, the upper surface of this unit has a relief of at least 4 m within the Parramore Island backbarrier. Therefore, these deposits form a topographically complex antecedent substrate upon which the Holocene barrier system has migrated. Notably, a substantial topographic high is identified between −5.5 and −6.0 m MSL along the landward margin of Parramore Island itself (Figs. 3, 4).

5.1.3. Unit III: Mid- to Late-Holocene lagoon fill

A package of fining-upward late-Holocene (≤5000 years old) sediment overlies the antecedent Pleistocene surface across the Parramore backbarrier. Finkelstein and Ferland (1987) described this unit as observed behind Hog Island (see location, Fig. 1) as Holocene high-energy lagoon deposits capped by fine, muddy tidal flat sediments. Newman and Munsart (1968) and Morton and Donaldson (1973) also mapped segments of this unit behind Parramore and Cedar islands. These sediments extend below modern Parramore Island, where they are found 3–4 m below the surface, even proximal to the modern beach (Fig. 3b). Generally very fine grained, with occasional beds of *Crassostrea virginica* (Eastern Oyster), Unit III-a is interpreted as backbarrier lagoonal fill. As first recognized by Finkelstein and Ferland (1987), the gradual upward-fining (silty sand to sandy silt and silt) trend commonly observed within this unit likely reflects a change from a higher energy (i.e., wide, open

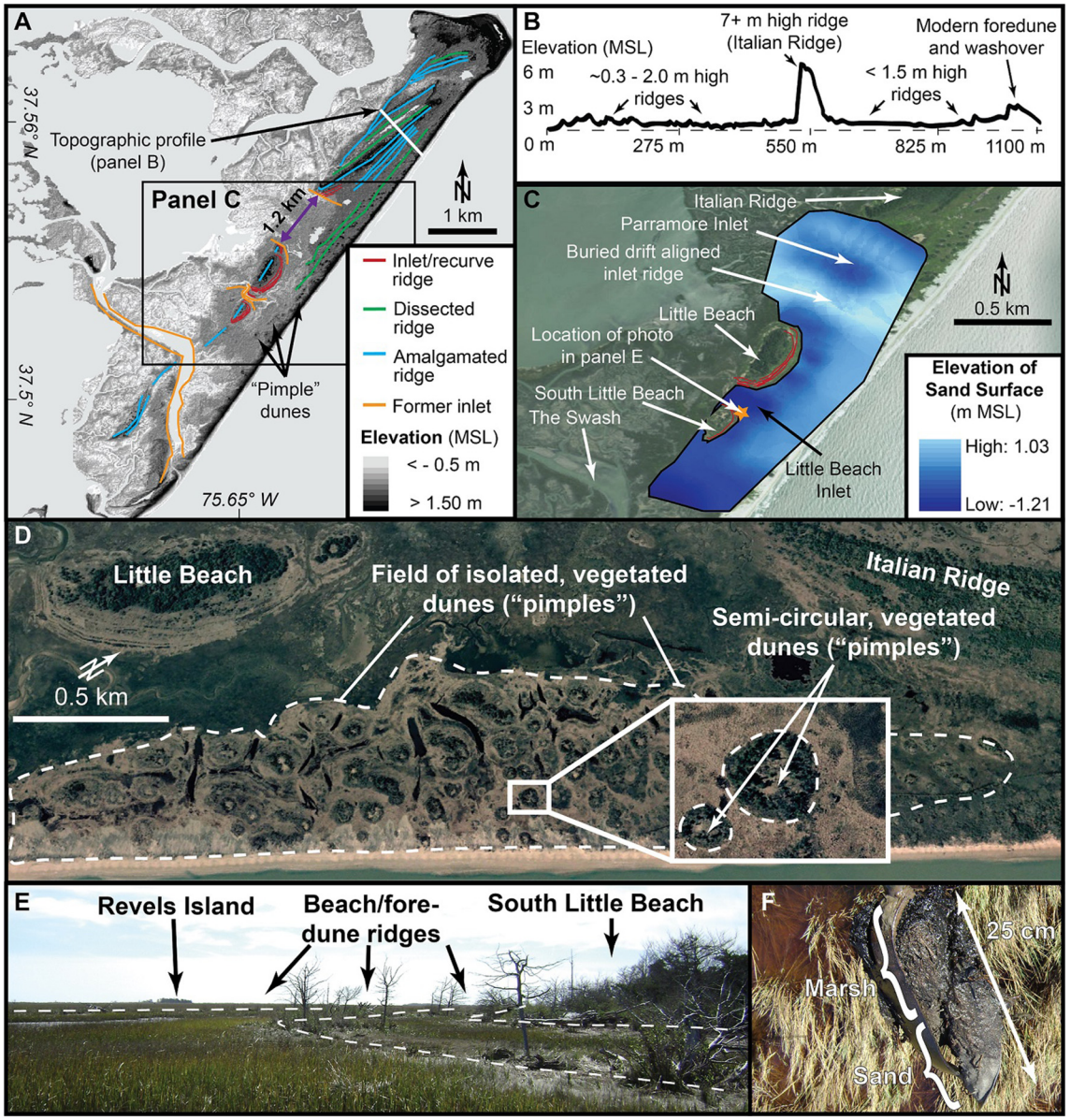

Fig. 6. Geomorphic mapping of Parramore Island. A) Ridges were traced and interpreted in ArcGIS using a LiDAR-derived digital elevation model from the CoNED Chesapeake Bay Topo-Bathymetric Map (USGS, 2016). Data below −0.6 m MSL were excluded to restrict bathymetric data. B) Shore-perpendicular topographic profile across Parramore Island showing variable ridge morphologies to the northwest and southeast of the 7+ meter-high Italian Ridge. C) Central Parramore interpolated lithostratigraphic sand surface. Auger core depth-to-sand data were corrected from RTK-GPS auger core elevations using known datums to obtain sand surface elevations. D) Aerial imagery showing the location of the field of isolated, vegetated dunes ("pimples") and two-dimensional morphology of selected "pimple" dunes (see photo insert). Imagery from Commonwealth of Virginia (2007). E) Annotated photo of South Little Beach ridge-and-swale system (see location, Fig. 6c). F) Field photo of auger core used for Little Beach swale mapping. Thin (generally ≤30 cm) saltmarsh overlies progradational ridge-and-swale sand in the interior of southern Parramore Island, between the modern foredune and Little Beach/South Little Beach/Revels Island.

lagoon) to a lower energy (i.e., narrow, marsh-filled lagoon) backbarrier environment. A radiocarbon sample from within this lagoonal fill (PARV10; Table 1) suggests this shift likely occurred between about 2000 and 3000 years ago.

Unit III-b, also mid-to-late Holocene in age, is interpreted as flood-tidal-delta sand and (minor) silt. The coarser nature of this sub-unit reflects the relatively higher energy proximal to tidal inlets. This sub-unit is found proximal to the barrier, and was mapped in detail proximal to Wachapreague Inlet by Newman and Munsart (1968). Elsewhere along the island, the presence of this unit is interpreted to reflect the occurrence of former proximal tidal inlet channels. For example, the fine sands found near Parramore Island in transect Y-Y′ (Fig. 4a) were most likely deposited by The Swash, an inlet active during the 20th century (see location, Fig. 6c).

5.1.4. Unit IV: Late-Holocene marsh

The abundance of organic material (including roots and rhizomes of *Spartina alterniflora* and *S. patens*) present in Unit IV supports its designation as the thin (≤1 m), late-Holocene saltmarsh unit that caps most backbarrier cores. A single radiocarbon date from immediately below the base of this unit indicates marsh may have formed as recently as ~400 years ago. The thin nature of the backbarrier marsh in the VBI was previously noted by Finkelstein and Ferland (1987), with specific examples from Parramore (Newman and Munsart, 1968) and Cobb islands (Oertel et al., 1989). Palynological data from the backbarrier of Parramore Island further indicates that central-backbarrier salt marsh formation began between 600 and 1000 years ago (Newman and Munsart, 1968). Finkelstein and Ferland (1987) provide similar dates (Supplemental Table 1) for initial extensive marsh formation

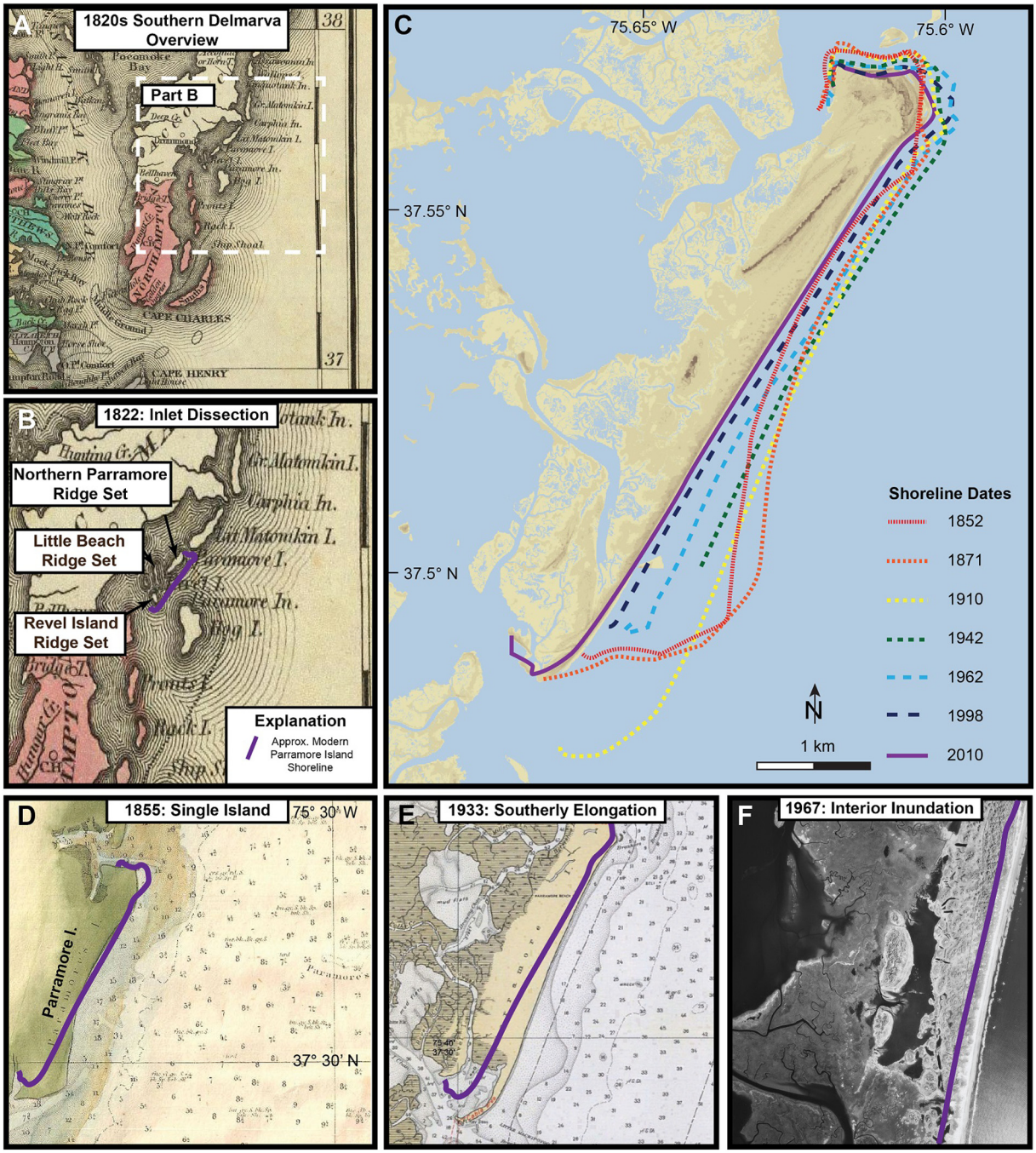

Fig. 7. Historical geospatial information. A) 1822 map of Virginia (Carey and Lea, 1822) showing broad-scale morphology of Virginia's barrier coast; panel B) provides a detailed view of Parramore Island from the same map. The map reveals dissection of Parramore by three inlets during the 18th and early 19th century; the positions of these correspond to breaks in large former foredune ridges located along western Parramore Island (i.e., Little Beach, South Little Beach, Revels Island; see locations, Figs. 1, 5). C) Historical shoreline data from Richardson (2012) showing late 19th Century progradation of southern Parramore and subsequent 20th and 21st century erosion of much of Parramore. The shoreline of northern Parramore is relatively stable, likely as a result of continued sediment delivery through inlet sediment bypassing and inlet-downdrift longshore sediment transport reversal. D) 1855 NOAA t-sheet (Chart Number: C-2-11, Preliminary Chart of Part of the Sea Coast of Virginia and Entrance to Chesapeake Bay) demonstrating inlet closure and the initiation of island progradation at the northern and southern ends. E) 1933 NOAA t-sheet (Chart Number: 1221, Chincoteague Inlet to Hog Island Light) showing erosion and southward elongation of southern Parramore. The Swash (a former inlet) along southern Parramore is re-directed to the south by Parramore's elongation. F) Farm Service Administration historical aerial photo (FSA ID: AR1SWBA00020058; coordinates: 37.53702°N, 75.62942°W; acquisition date: 13-Jan-67; scale: 20500) of central Parramore Island in 1967, showing tidal inundation of the swale eastward of Little Beach and South Little Beach. The approximate location of the modern shoreline of Parramore Island (purple line) is shown in (B), (D), (E), and (F). (For interpretation of the references to color in this figure legend, the reader is referred to the web version of this article.)

throughout the VBI backbarrier, including at Assawoman (610 ± 73 and 655 ± 91 cal. years BP), Hog (456 ± 159 cal. years BP), and Metompkin islands (1108 ± 147 and 1565 ± 166 cal. years BP). Closer to the mainland, Newman and Rusnak (1965) date basal peats from this unit to 2238 ± 185 cal. years BP (Supplemental Table 1). Likewise, cores from this study reveal thin (generally < 50 cm) segments of peat within Unit III lagoonal fill deposits, some of which (e.g., that found at the bottom of PARV04 (Fig. 3a)) date to 4835 ± 65 cal. years BP.

5.1.5. Unit V: Barrier island and shoreface sediments

The textural and mineralogical maturity of sands, and the presence of shells and shell hash in components of Unit V, are characteristic of barrier island and shoreface environments. As such, several sub-units together compose the barrier island proper: Unit V-a, beach and shoreface sands; Unit V-b, washover deposits; Unit V-c, inlet fill; Unit V-d, aeolian dune ridges; and Unit V-e, marsh-filled swales.

The dominantly medium-sized, quartz-dominated sand containing abundant shells and/or shell fragments are interpreted as shoreface and beach sands (V-a) and form the base of the barrier-island sediments in the eastern 90% of the island.

Washover deposits (V-b) are found along the landward edge of Parramore Island along much of its extent (e.g., PARV18, PARV24, and PARV25 in Fig. 4b). An in situ articulated *Crassostrea virginica* (Eastern Oyster) shell (see PARP01, Fig. 1d) provided a maximum age of 989 ± 180 cal. years BP for the overlying washover deposit (Unit V-b). This species is common to shallow-water, low-energy backbarrier environments, and this particular specimen—collected from within a dense bed of *C. virginica* shells—was likely buried by sand overwashed onto a former backbarrier intertidal flat. These washovers are interpreted as late-stage transgressive deposits marking the landward-most position of Parramore Island.

Ridges east of these washover deposits consist primarily of medium sand, interpreted as beach ridges (V-a), and overlying fine sand, interpreted as aeolian dune ridges (V-d). Cores collected in the swale immediately west of Italian Ridge (PARV01 and PARG02) and west of the modern foredune ridge (PARG03, Fig. 3b) contain identical beach and shoreface sand < 0.3 m below the surface. Together, these form the core of the progradational beach- and dune-ridge systems of the barrier island. Seaward-dipping reflectors in GPR data (Fig. 5) indicate that Italian Ridge and Little Beach built as a series of beach ridges which were later capped by aggradational aeolian deposits; this same process was likely responsible for the development of all ridges observed on Parramore Island. OSL dates (Table 2) indicate that the ridge set composing Revels Island was active until ~500 years ago, while at least the aeolian components of Italian Ridge, Little Beach, and a dune ridge on the northwestern end of the island (see OSL sampling locations, Fig. 1) were actively developing up to ~150 years ago. These dates are supported by historical maps, which indicate that Parramore Island reached its maximum extent at ca. 1870 (Fig. 7c). Furthermore, these dates align with estimates for Hog Island, which Harris (1992) determined is only 200–300 years old in its present morphological configuration.

The ridges of Unit V-d are dissected by a series of at least three paleo-inlets (V-c): (1) Parramore Inlet, located between the southern terminus of Italian Ridge and Little Beach; (2) Little Beach Inlet, located between Little Beach and South Little Beach; and (3) The Swash, separating Revels Island from Parramore Island proper. Of these, Parramore Inlet and The Swash are identified by name on historic maps. These same maps also show the segmentation of Parramore Island into at least three smaller islands (Fig. 7b). Inlet-fill sequences, such as that recorded in core PARG07 (Fig. 4a), are recognized to be a dominant component of barrier-island lithosomes (Moslow and Heron, 1978; Moslow and Tye, 1985; Tye and Moslow, 1993; FitzGerald et al., 2001). For example, inlet fills represent a significant portion of stratigraphic architecture of wave-dominated Assateague Island, located 45 km north of Parramore (Seminack and Buynevich, 2013; Seminack and McBride, 2015). The same type of morphological features which are well preserved on Assateague, such as sets of recurve and inlet-closure ridges located adjacent to the ~1 km wide Sinepuxent Inlet (active 1755–1832) (Seminack and McBride, 2015), are visible along the periphery of Little Beach and South Little Beach (Fig. 6e).

Unit V-e, an organic-rich sub-unit of the barrier-island complex, is interpreted as young (< 100 years) marsh that has recently migrated into the swales between ridges on Parramore Island. Despite its distinct biofacies, the very fine to fine sand lithofacies of the unit is sedimentologically similar to the rest of Unit V, reflecting the proximity of dune and swale sediment sources to the marsh.

5.2. Mid- to Late-Holocene evolution of Parramore Island

5.2.1. Initial barrier-island formation during the Middle Holocene

The morphology of the Pleistocene substrate underlying the VBI derives from the stacking and reworking of sediments in response to a series of glacial-interglacial transgressions and regressions (Demarest and Leatherman, 1985; Krantz et al., 2016). As sediment was driven landward during the Holocene transgression, it was deposited atop dendritically incised Pleistocene headlands. In this manner, barrier islands became “pinned” to topographic highs between river channels and continued to accrete in response to sediment reworking and RSLR (Demarest and Leatherman, 1985).

The presence of mainland-fringing saltmarsh, as well as the deposition of backbarrier lagoonal sediments, along an otherwise open-ocean Virginia coast, indicates the presence of fronting barrier islands no later than the middle Holocene. Finkelstein and Ferland (1987) interpreted the presence of saltmarsh (*Juncus*) peat at −7 m MSL behind Metompkin Island as evidence that barrier islands were present offshore of their current locations by ca. 4600 years ago. Calibration of this marine date (Supplemental Table 1) reveals that initial barrier-island formation occurred ~700 years earlier (5348 ± 266 cal. yrs BP). Although the oldest date from this study for marsh growth behind Parramore Island is younger (4835 ± 65 cal. yrs BP; Table 1), it is likely that initial upland flooding, formation of saltmarsh, and the deposition of backbarrier sediments within the area now occupied by the Parramore Island backbarrier began > 5000 years ago. Together, these findings support earlier conclusions (e.g., Finkelstein and Ferland, 1987) that the VBI formed several kilometers offshore of their present location by the mid-Holocene, likely as a series of small, proto-barriers that migrated landward across exposed Pleistocene uplands.

5.2.2. Barrier-island pinning and stabilization: the role of antecedent substrate

Following initial formation, Parramore Island retrograded to a position corresponding to the western side of the large beach/dune ridges on its northern end (Fig. 8a). It reached this position by ca. 1000 years ago, as evidenced by washover deposits found overtopping in situ *C. virginica* in northern Parramore. This relative sequencing of deposits matches well with that identified along the southwestern side of Hog Island, where radiocarbon analyses from peat samples and in situ shells (*Mercenaria campechiensis*) from an underlying shell bed date to about 1100 years BP and 1400 years BP (re-calibrated ages), respectively (Rusnak et al., 1963; Harrison et al., 1965). Rice et al. (1976) interpret these as evidence of an earlier, overwash-dominated “proto-Hog Island”. The presence of washover sands overtopping marsh and lagoon sediments west of both Western Ridge (Fig. 3b) and Little Beach (Fig. 4b) indicates that Parramore Island was once similarly overwash-dominated. Together, these data also indicate that retrogradation of both Parramore and Hog islands continued until about 1000 years ago, when both stabilized in their landward-most positions.

The stabilization of proto-Parramore Island (Fig. 8b) occurred at a time of gradually slowing RSLR (Fig. 2), when sand fluxes along this generally sediment-starved coast first matched or outpaced the rate of accommodation creation. However, the location at which the island stabilized, and thus the exact timing of its halting migration, may well reflect underlying geologic controls. Antecedent topography and substrate lithology can control the development and migration rates of barrier-island systems by providing the regional slope (e.g., steep cliffs versus shallow coastal plain) over which coastal systems migrate during transgression (Belknap and Kraft, 1985). More localized influences on barrier-island evolution are two-fold: antecedent geology controls the slope over which an island migrates, as well as the nature (i.e., sand, mud) and availability of sediment to the longshore sediment-transport

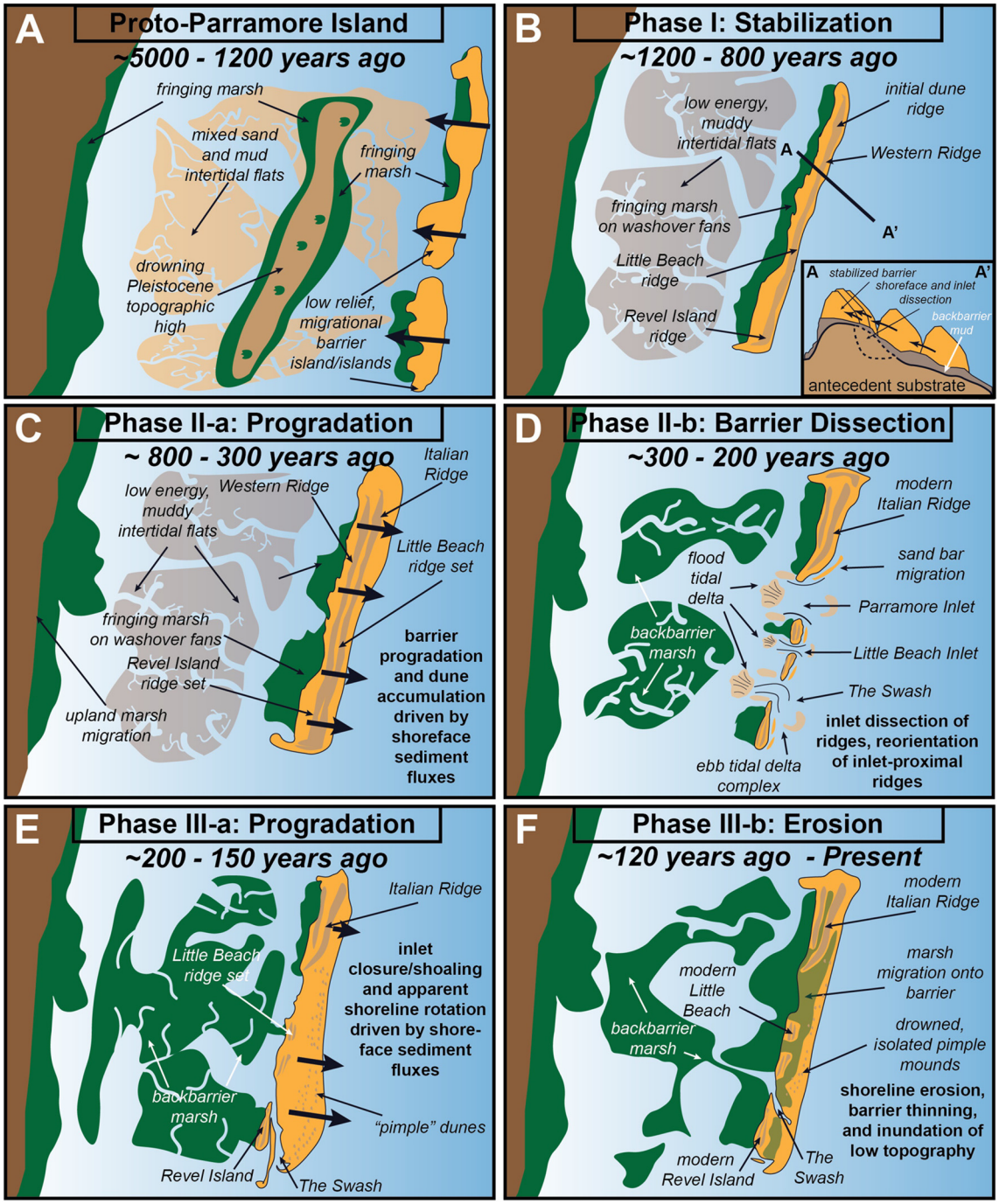

Fig. 8. Conceptual evolutionary model of Parramore Island. A) Proto-Parramore, first formed > 5000 years ago, was a low-profile, overwash-dominated, landward-migrating barrier island (or set of islands). The early lagoonal sediments deposited in the backbarrier of Parramore Island are silt-rich, reflecting higher energy from a more open lagoon. B) *Phase I: Stabilization* Parramore Island stabilizes in response to pinning and sediment delivery from a combination of antecedent slope and sandy antecedent substrate. C) *Phase II-a: Progradation* A period of early barrier progradation begins, likely driven by increased shoreface sediment fluxes. D) *Phase II-b: Barrier Dissection* Following initial progradation, multiple inlets breached the ridges, possibly in response to an extended period of enhanced storminess. E) *Phase III-a: Inlet Closure and Progradation* Shoreface sediment fluxes, perhaps originating in part from excavation from the sandy antecedent substrate by multiple tidal inlets initiated a 100–200-year period of progradation. F) *Phase III-b: Erosion* Parramore has undergone erosion throughout much of the 20th and 21st centuries (accelerating in recent decades), likely in response to both reduced alongshore sediment supply and a late-20th-Century acceleration in relative sea-level rise.

system (e.g., Rodriguez et al., 2004; Moore et al., 2010; Timmons et al., 2010; Brenner et al., 2015). The control of antecedent geology and topography on barrier-island behavior has been observed in a range of coastal settings, including Delaware (Belknap and Kraft, 1985), east Texas (Rodriguez et al., 2004), west Florida (Davis and Kuhn, 1985), North Carolina (Riggs et al., 1995;Timmons et al., 2010; Zaremba et al., 2016; Mallinson et al., 2018), and Georgia (Oertel, 1979). Additionally, numerical modeling studies of Moore et al. (2010), Lorenzo-Trueba and Ashton (2014), Brenner et al. (2015), and Ashton and Lorenzo-Trueba (2018) have demonstrated the complex influences on barrier-island migration processes of variable backbarrier slope and sediment type.

Along the Virginia Atlantic coast, antecedent topographic highs associated with earlier highstands of sea level are surficially exposed in the form of Mockhorn Island (Finkelstein and Kearney, 1988) and

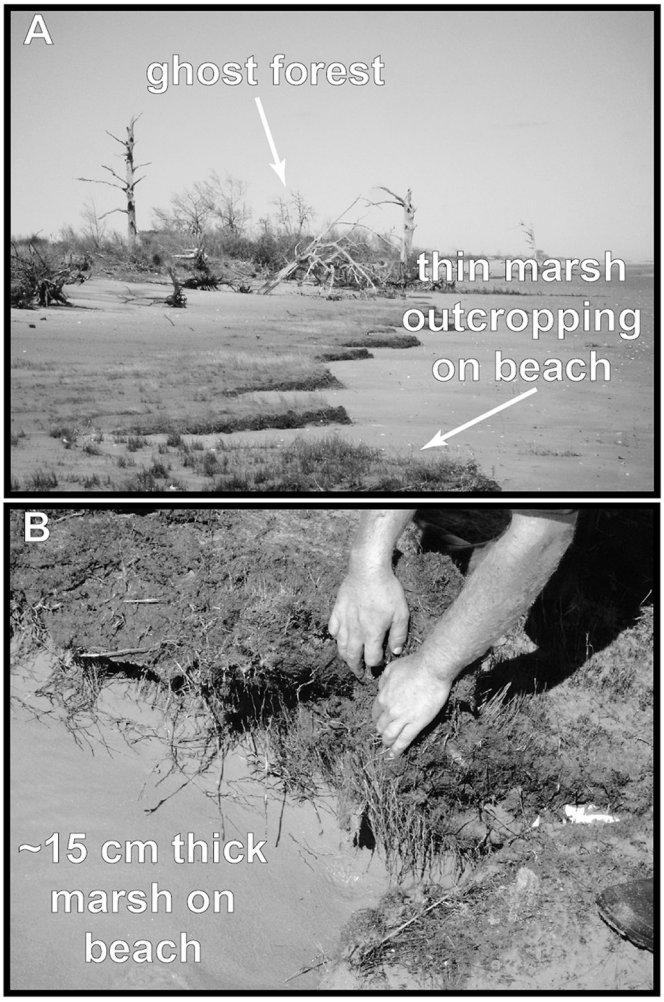

Fig. 9. Erosion of former beach/foredune ridges and swales along Parramore's central shoreline. A) Northward-looking photo from central Parramore beach. Note peat outcrops in the surf zone (foreground), erosional scarp in mid-field, and "ghost forests" in the distance. B) Peat outcrops eroded along the ocean side of Parramore Island are from thin (generally ≤30 cm), young marsh formed atop Parramore Island following 19th century progradation, growth of seaward ridges, and drowning of interior swales.

Upshur Neck (Halsey, 1978), and have either been observed, or hypothesized to exist, at shallow depths proximal to the landward sides of Cobb, Smith, and Hog islands (Oertel et al., 1989; Harris, 1992). New sediment cores from across Parramore Island (Figs. 3, 4) demonstrate the presence of this same buried topographic ridge (Unit II) buried at −6 m MSL below western Parramore Island. Parramore Island is not situated directly atop this ridge, as fine lagoonal and saltmarsh deposits vertically separate units II and V. It is thus likely that this ridge was subaerially exposed as a backbarrier island as recently as 4000 years ago. It was later buried within the lagoon fill as RSL rose. Nonetheless, this compact, sandy sediment (Unit II) may have provided a pinning and stabilization point for the migrating island. Moreover, the transgressing shoreface and subsequent inlets (see Section 5.2.3) likely dissected the sandy antecedent substrate, providing a local sediment source to the developing island. These field findings are consistent with outcomes of the morphokinematic models of Moore et al. (2010), which show that barrier-island migration may slow in response to sediment delivery from shoreface erosion of sandy substrate.

5.2.3. Barrier-island progradation and barrier dissection: the role of sediment fluxes and storms

Following pinning and stabilization, proto-Parramore shifted to a phase of progradation (Fig. 8c), likely reflecting a combination of slow RSLR and an abundance of sediment delivered both alongshore and cross-shore. This phase is characterized by the growth of successive beach and foredune ridges that may have formed as a series of landward-migrating offshore bars associated with sediment-bypassing processes along proximal tidal inlets (i.e., Wachapreague and Quinby inlets). A similar mechanism of barrier-island growth has been suggested for barrier islands such as Kiawah Island, South Carolina (Moslow, 1980), Sanibel Island, Florida (Missimer, 1973), and the East Friesian Islands, Germany (FitzGerald et al., 1984).

The longevity of the period of island progradation is unclear; it is possible Parramore remained a stable, narrow island for several hundred years following the halting of retrogradation. However, morphologic, chronostratigraphic, and historical data indicate that, following initial progradation, Parramore was segmented into at least four smaller barriers (Fig. 8d), a configuration retained until about 200 years ago. The large, shore-parallel dune ridges preserved on Revels Island, South Little Beach, Little Beach, and north-central Parramore are hypothesized to have once been a single, continuous shore-parallel ridge. Dissection of this continuous ridge through breaching and formation of multiple tidal inlets, each 200–1000 m in width and perhaps 9 m or more in depth (see PARG07, Fig. 4a), may have been associated with enhanced storminess during at least part of the period between 1000 and 200 years ago. Such a mechanism has been implicated in the partial deterioration of the wave-dominated North Carolina barrier islands during both the Medieval Climate Anomaly (ca. 1200–800 cal. years BP) and the Little Ice Age (ca. 500–200 cal. years BP); the resulting inlets had largely closed by the early 1800s (Mallinson et al., 2011, 2018). These same periods of enhanced mid-Atlantic storminess, documented in morphological (e.g., Wright et al., 2018) and paleotempestological (e.g., Donnelly et al., 2015) records throughout the western North Atlantic may also have been responsible for at least one phase of breaching and segmentation of Parramore Island in the pre-historic period.

Historical maps show Parramore Island as multiple separate barrier islands until about 200 years ago (Fig. 7b). Alongshore migration of associated inlets eroded large parts of former dune ridges. For example, a > 1 km wide swath of low topography between southern Western/Italian Ridge and Little Beach may be associated with the alongshore migration of the former (historical) Parramore Inlet; the dimensions and morphology of the resulting inlet-fill are comparable to those of the former Sinepuxent Inlet on Assateague Island (Maryland; active 1755 to 1832 CE; Seminack and McBride, 2015). Ultimately, these inlets began to fill, with eventual closure facilitated by downdrift beach accretion across inlet mouths. A series of closely spaced, 0.5 m high, drift- and swash-aligned ridges near Little Beach and the southern terminus of Italian Ridge (Fig. 6a) are associated with inlet closure. The well-documented historical (early 1900s CE) development of the VBI's Fisherman Island (located at the mouth of Chesapeake Bay; see Fig. 1) provides an analog for this island amalgamation process (Oertel and Overman, 2004).

5.2.4. Historical state shifts: transitions between progradation, rotation, and erosion

Upon inlet closure, Parramore Island entered a second phase of progradation and southerly elongation (Fig. 8e). During the 19th century, at least four dune ridges, ranging in height from 0.7 to 1.1 m, and generally spaced ~75 to 100 m apart, built seaward of Italian ridge on northern Parramore Island. To the south, a wide swale and multiple low-profile beach and dune ridges built seaward of Little Beach; the remnants of one of these form the core of the modern erosional foredune of central Parramore Island (Fig. 9a). At its southern end, Parramore elongated, building a recurved spit in front of Revels Island

(Fig. 7e). Growth of Parramore Island continued until the 1870s, when it reached its maximum width, which exceeded 1.5 km at its southern end (Figs. 7c, 8e).

Based on historical shoreline-change mapping, Parramore Island, along with Hog and Cobb islands, has traditionally been labeled a "rotational" barrier island. Richardson (2012) shows that Parramore has been largely stable to the north (Newman and Rusnak, 1965; Harris, 1992), with erosion on its southern end (nearly 1 km between 1852 and 2010) leading to perceived rotation of the island between the late 19th and middle 20th centuries (Fig. 7c). The stability and/or limited progradation observed at the island's northern end is the result of high sediment fluxes through bar welding associated with inlet bypassing around Wachapreague Inlet (McBride et al., 2015). However, since 1950, northern Parramore has started to erode, leading to an acceleration in island-wide shoreline retreat from a long-term (1850–2010) rate of 4.5 m/yr to > 12 m/yr since 1980 (Deaton et al., 2017). This apparent shift to a phase of parallel island retreat (Richardson, 2012; McBride et al., 2015) has been attributed to a combination of complex sediment-transport and sediment-trapping (particularly of coarser sands) dynamics associated with the growth of Fishing Point (southern Assateague Island; Fig. 1a; Finkelstein and Ferland, 1987; Wikel, 2008; Richardson, 2012; Fenster and McBride, 2015) and the Wachapreague Inlet ebb-tidal delta (e.g., Richardson, 2012; Fenster et al., 2016), and possibly periods of enhanced storminess in the late 20th century (Fenster et al., 2017). Continued retreat could extend the Arc of Erosion south to incorporate Parramore Island (Richardson, 2012; McBride et al., 2015; Deaton et al., 2017).

5.2.5. Interior island inundation

Whereas RSLR may be among the contributing factors to the recent (last 150 years) shift of the Parramore Island shoreline to rapid erosion, it is the sole cause of two other significant changes observed in the interior of Parramore Island: ridge segmentation and swale drowning.

The interior of Parramore Island is characterized by vegetated, semi-circular isolated "pimple" dunes which are 10–20 m in diameter and 0.7–1.5 m high (Fig. 6d; McMillan and Day, 2010). These features are interpreted to be associated with the destructive phase of progradational beach/foredune ridges; that is, remnants of continuous, hummocky foredune ridges, formed initially through aeolian processes and later segmented through partial drowning by RSLR. Hummocky ridges develop as non-continuous/non-amalgamated incipient dunes formed when relatively rapid progradation starves the dune of sediment from the beach, preventing it from coalescing (Ruz et al., 2017) Isolated dunes persist if lateral vegetation growth rates do not outpace inundation recurrence intervals (Goldstein et al., 2017). Eco-geomorphic feedbacks, such as the growth of grass, shrubs, and woody vegetation, which trap sediment in the interior of dunes, as well as wash-around, which erodes the perimeter of dunes, allows for the persistent semi-circular morphology of "pimple" dunes (Hayden et al., 1995; McMillan and Day, 2010; Stallins and Corenblit, 2017). On Parramore, many of these pimple dunes have become fully isolated by continued RSLR, but groups retain orientations suggestive of their origin as hummocky foredune ridges.

By 1950, the interior sandy swale of central Parramore (separating Little Beach and South Little Beach from the larger ridges to the east) had been entirely drowned (Figs. 6c, 7f), leaving only sparse "pimple" dunes along its seaward margin (Fig. 6d). This area was subsequently occupied by expansive (covering an area of ~3.5 km^2), thin (average: ~25 cm; see Fig. 6c, f) muddy tidal flats and low marsh *S. alterniflora*. This island-interior marsh expansion partially countered some of the ~18 km^2 of backbarrier marsh lost (largely to edge erosion) behind Parramore Island between 1870 and 2010 (Deaton et al., 2017). However, recent, rapid narrowing of Parramore Island may threaten marsh stability (and the carbon stored therein) as the young, thin marsh covering former swales becomes exposed on the shoreface (Fig. 9). A radiocarbon date of this marsh exposed along the shoreface of northern Parramore (PARA03; Table 1; see location, Fig. 1) confirms the very young age (post-1950) of this eroding intra-swale marsh. Along higher-elevation ridges, barrier-island retreat also has led to die-offs of Parramore's extensive forests from exposure to saltwater on the shoreface (McBride et al., 2015; Fig. 9a). Given future projected rates of RSLR along the Virginia coast (Boon and Mitchell, 2015), further deterioration of these barrier-island ecosystems is likely.

5.3. Implications for barrier-island stability in the face of changing climate

5.3.1. Youth of Parramore Island

Ages provided by OSL and radiocarbon analyses reveal that Parramore Island—and likely other barrier islands within the VBI system (e.g., Hog Island)—is substantially younger (at least in its modern position) than many others across the U.S. East and Gulf coasts. For example, Galveston Island (Texas), widely considered an archetype of progradational barriers (Bernard et al., 1959; Morton and Price, 1987; Morton, 1994), initially began building around 5300 years ago (Rodriguez et al., 2004). Shells from transgressive deposits (capped by shoreface sediments) in the backbarrier of Kiawah Island (South Carolina) date to 4400 and 4500 years BP (Moslow, 1980; Duc and Tye, 1987). In New England, Plum Island (Massachusetts), which is almost entirely progradational and elongational, stabilized at its modern location by 3600 years ago (Hein et al., 2012). The Georgia Bight barriers, while commonly containing a Pleistocene core, feature Holocene progradational ridges, which likely began forming 4000–5000 years ago (Hayes, 1994). Additionally, changes in foraminifera assemblages in sediment cores from Pamlico Sound, North Carolina indicate that the Outer Banks had formed in their near-modern location (also perched on a Pleistocene high) by ca. 3500 years BP (Culver et al., 2007), and that at least parts of the modern systems (e.g., prograding beaches of Kitty Hawk (Mallinson et al., 2008; Moran et al., 2015), flood-tidal deltas of Bogue Banks (Lazar et al., 2016)) had been emplaced between 4000 and 6000 years BP.

In contrast, Parramore and Hog islands, which likely existed offshore by at least 5000 years ago, did not reach their present location until the last 1200 years. In this manner, the onset of progradation on Parramore Island (and likely Hog as well, though no detailed data exist for its pre-historic record of progradation) aligns with the regressive growth of Saint Joseph Peninsula, the youngest barrier feature (< 1000 years old) in Florida's Apalachicola Barrier Island Complex (Rink and López, 2010). However, the remainder of the Apalachicola barrier system is much older, dating to ca. 3000 years old (Rink and López, 2010), and is therefore more comparable to the ages of other progradational U.S. Atlantic and Gulf Coast barrier islands. Thus, at least in their present configuration, it is likely that even the oldest, progradational/rotational VBI (Parramore, Hog) may be among the youngest "stable" (i.e., non-migrating) barrier islands on the U.S. Atlantic and Gulf coasts. This likely reflects the complex interplay between RSLR, antecedent substrate, and alongshore sediment delivery in the VBI system.

5.3.2. Late Holocene VBI sediment delivery mechanisms and progradation rates

Beach and foredune ridges, among the most prominent features on Parramore Island, are most pronounced proximal to modern and paleo tidal inlets (Figs. 1, 6). Such inlets often control proximal shoreline behavior (erosion vs. accretion) along barrier islands, largely because of associated wave- and tide-driven inlet-sediment-bypassing and bar-welding processes (FitzGerald, 1984; FitzGerald et al., 1984; Fenster and Dolan, 1996). Given the slow long-term growth rate of northern Parramore (1300 m in ~1000 years), it is likely that most sediment delivered to northern-most Parramore through processes associated with Wachapreague Inlet continued to be reworked alongshore to the south, aiding in two major phases of overall island progradation. Following stabilization of the landward-migrating proto-Parramore

~1000 years ago, northern Parramore prograded approximately 600 m in ≤800 years (~0.8 m/yr). Historical shoreline data, paired with the OSL date from Italian Ridge, indicate rapid progradation (~6 m/yr) of northern Parramore Island (along transect X–X′ of Fig. 1) beginning at ca. 200 years ago and ending ca. 75 years ago. Likewise, a simple linear transect from Revels Island (southern Parramore) to the maximum historical shoreline position indicates similar rapid progradation (~7 m/yr) starting ca. 560 years ago and ending ca. 150 years ago. This period of accelerated growth around 200 years ago may have been associated with a higher net sediment fluxes to Parramore Island, possibly related to ebb-tidal delta dynamics at Wachapreague and Quinby inlets, or increased longshore sediment transport. Alternatively, this change in shoreline behavior may have been in response to the period of slower RSLR following the Medieval Warm Period (Kemp et al., 2011).

The high average height of Italian Ridge (up to 7 m above MSL) may indicate a longer period of active foredune accretion and a decrease in the rate of coastal progradation. This observation is consistent with the conceptual theory that, as sediment availability decreases, beach progradation slows, and the volume of the active foredune increases (Psuty, 2008). It also follows observations from a number of global progradational systems (e.g., Usumacinta-Grijalva beach-ridge plain, Mexico (Nooren et al., 2017), Guichen Bay beach-ridge plain, Australia (Bristow and Pucillo, 2006), North Island spit, South Carolina, USA (Wright et al., 2018)), in which shoreline progradation rates are shown to be inversely related to dune ridge elevations as a function of sediment supply. Given its higher relative elevation, Italian Ridge may similarly indicate a period of slower shoreline progradation While decreased progradation rates may be linked to increased accommodation as the barrier island builds seaward into deeper water, the relatively flat stratigraphic contact between shoreface sediments and underlying sediments (Figs. 3, 4) instead indicates that changes in sediment supply (both delivery through long-/cross-shore transport, and erosion by storms) controlled changes in the progradation of Parramore Island. Therefore, an additional, much lower, sediment supply regime corresponding with the growth of Italian Ridge may have existed between ~1000 and ~200 years ago, but the exact interval cannot be constrained with available data.

The 20th century marked a period of widespread island erosion, likely in response to reduced sediment supply, or the recent increase in the rate of RSLR; even faster periods of island erosion have been linked with decadal periods of increased storminess (Fenster et al., 2017). Yet, this same accelerated erosion into the 4–6 m thick sandy barrier lithesome liberates sediment that can then be transported south by the wave-driven longshore transport system, possibly increasing the sediment flux to Hog Island. Indeed, Hog is the only island of the mixed-energy VBI (excluding Wallops and Fisherman islands: the former is nourished and the latter is at the southern sediment sink for the system) which has undergone net progradation (which followed a longer period of erosion) in the last 35 years (Deaton et al., 2017).

5.3.3. Barrier-island dynamics: stability and state changes in response to changing environmental conditions

Documented regime shifts between phases of retrogradation, progradation, segmentation, and erosion underscore the complex and interconnected nature of Parramore Island's response to changes in RSL, sediment supply, and storm impacts. The earliest evidence for the existence of Parramore Island is the presence of backbarrier marsh and lagoonal sediments. Parramore Island first formed by at least 4835 ± 65 cal. yrs BP, coinciding with a period of apparent deceleration in RSLR (Fig. 2). Stabilization and phase shift of Parramore Island to progradation occurred following a second apparent deceleration in RSLR from a time-averaged rate of 1.6–1.7 mm/ yr to ca. 1 mm/ yr at ca.~1500 cal. yrs BP (Fig. 2, Supplemental Table 1). Transitions from net transgression (erosion and/or retrogradation) to net progradation of sandy coastal systems (including barrier islands and beach-ridge plains) have been documented globally as RSLR has decreased below similar threshold RSLR rates; these vary from ~2 mm/ yr in Brazil (Hein et al., 2014) and the Danish North Sea (Fruergaard et al., 2015); to ~1.3–1.5 mm/ yr in Massachusetts (Hein et al., 2012) and Newfoundland (Billy et al., 2015); to as low as 0.8 mm/ yr in North Carolina (Timmons et al., 2010) and 0.4 to 0.6 mm/ yr in Texas (Anderson et al., 2016). The lower rate of RSLR required for transitions to progradation in sites distal from abundant (in particular, fluvial) sediment sources, such as North Carolina and Virginia, likely reflects the critical role of sediment fluxes to the coast.

The Virginia coast has experienced a significant acceleration in RSLR in the last two centuries, reaching approximately 5 mm/ yr since the 1960s (Boon and Mitchell, 2015). This coincided with a multi-decadal transition of Parramore from growth to erosion, as well as the acceleration in erosion/migration observed along the VBI more generally (Deaton et al., 2017). Together, these findings add further evidence for the existence of a threshold rate (despite local variability in upland slope, erodability of antecedent substrate, and alongshore sediment supply rates; see Hein et al., 2014 for complete discussion) of RSLR beyond which even formerly progradational sandy coastal systems become destabilized and transition to periods of erosion and, in the case of barrier islands, landward translation. This rate may well have been surpassed > 100 years ago along the VBI coast.

An alternative, though not mutually exclusive, hypothesis for the recent transition of Parramore toward rapid erosion is a reduction in the rate of longshore sediment delivery. A common, though as yet unproven, hypothesis for the causal mechanism for the rapid erosion/migration of the northern VBI (the “Arc of Erosion”: Assawoman, Metompkin, and Cedar islands) is the accumulation of sediment at the recurved spit of Assateague Island (“Fishing Point”) (Leatherman et al., 1982; Richardson, 2012; Fenster and McBride, 2015; Fenster et al., 2016). Similar barrier-island shoreline changes are observed in response to variations in sediment supply associated with the tidal-inlet channel and bar dynamics (FitzGerald, 1984, 1988; Elias and Van Der Spek, 2006; Fallon et al., 2015), sediment trapping at updrift spits (Park and Wells, 2007), and sediment trapping and bypassing of coastal reentrants and estuaries (Anthony, 1995).

Considering these examples, an allogenic, sediment-supply driven cascading effect is postulated along the VBI: in the short term (tens of years), rapid erosion of the Parramore Island lithosome will allow for continued delivery of excess (beyond the net littoral longshore sand pass-through) sediment to Hog Island by longshore transport. However, once Parramore Island narrows to the point at which it breaches and becomes overwash-dominated, the island will migrate landward, shifting dominant sediment transport from longshore to cross-shore, reducing southerly longshore sediment fluxes and starving downdrift barrier islands. This is anticipated to result in a transition to net erosion along Hog Island (historically the most stable progradational island within the VBI system), and the initiation of a multi-decadal conversion of Hog Island toward overwash-dominated, in the same manner as that observed along Parramore. We hypothesize that this same sequence of events may have been partially responsible for variations in sediment fluxes to Parramore Island, as Cedar Island underwent similar phase shifts during the last 1000 years; however, present data do not allow for further exploration of this theory.

6. Conclusions

This study presents new stratigraphic, sedimentologic, chronologic, geophysical, morphological, and historical data from one of the largest barrier islands in the Virginia Atlantic coast barrier-island chain. The complex late-Holocene evolution of Parramore Island emphasizes the inter-connected roles of antecedent geology, sea-level rise, storms, and sediment supply to control the relative stability of mixed-energy barrier islands. In particular, it reveals the following:

1. Parramore Island originally formed > 5000 years ago and migrated

landward in response to relatively low RSLR rates (~1.6 mm/ yr).
2. Landward migration of Parramore Island ended approximately 1000 years ago due in part to stabilization associated with the pinning point and erosional sediment source provided by antecedent substrate.
3. The first phase of island progradation initiated ~1000 years ago during a period of slow RSLR (~1 mm/ yr), closely corresponding to rates of sea-level rise associated with the natural shift from landward migration/erosion to progradation of other regional and global barrier systems (both prograded barriers and barrier islands).
4. During a phase otherwise characterized by net progradation, Parramore Island underwent periods of segmentation around ~300–400 years ago, corresponding to a period of heightened Mid-Atlantic cyclone activity.
5. Recent (~150 years) of erosion of Parramore Island is in response to a combination of reduced longshore sediment fluxes and/or increased rates of RSLR.
6. It is possible that barrier-island state transitions from erosional (providing sediment to downdrift barriers) to migrational (dominated by onshore sediment fluxes) starve downdrift barriers of a former sediment source, causing them to shift from stability or progradation to erosion and eventual retrogradation. Along natural, multi-island barrier systems such as the VBI, this may result in a downdrift-cascading net sediment deficit that can lead to gradual system-wide destabilization and transition toward rapid transgression during a period of accelerated RSLR.

Supplementary data to this article can be found online at https://doi.org/10.1016/j.margeo.2018.04.007.

Acknowledgements

Funding was provided by the Mid-Atlantic Regional Sea Grant Program (NOAA) award numbers R/71856G & R/71856H and the Virginia Institute of Marine Science's (VIMS) Eastern Shore Lab scholarship. J. Shawler was supported by the VIMS School of Marine Science Office of Academic Studies and the VIMS Harry and Barbara Hager Fellowship. We thank S. Johnson for partial support of the R/V Peregrination. We thank J. Connell, S. Baker, and K. Brown for their field and laboratory assistance. S. Fate, P.G. Ross, E. Smith, A. Birch, K. Gedan, A. Greene, B. Pfirrman, J. Krask, J. Perry, A. Janoff, C. Drake, M. Fenster, and J. Vaughn provided additional field support. E. Chamberlain contributed to discussions of OSL interpretations. We thank two anonymous reviewers for their thorough review of this work. We appreciate the permissions granted by The Nature Conservancy and the Virginia Marine Resources Commission. This paper is Contribution No. 3738 of the Virginia Institute of Marine Science, College of William & Mary.

References

Aitken, M.J., 1985. Thermoluminescence Dating. Academic Press, New York.
Aitken, M.J., 1998. An Introduction to Optical Dating: The Dating of Quaternary Sediments by the Use of Photon-stimulated Luminescence. Oxford University Presshttp://dx.doi.org/10.1002/(SICI)1520-6548(200001)15:1<81::AID-GEA5>3.3.CO;2-Y.
Anderson, J.B., Wallace, D.J., Simms, A.R., Rodriguez, A.B., Weight, R.W.R., Taha, Z.P., 2016. Recycling sediments between source and sink during a eustatic cycle: systems of late Quaternary northwestern Gulf of Mexico Basin. Earth-Sci. Rev. 153, 111–138. http://dx.doi.org/10.1016/j.earscirev.2015.10.014.
Anthony, E.J., 1995. Beach-ridge development and sediment supply: examples from West Africa. Mar. Geol. 129, 175–186.
Ashton, A.D., Lorenzo-Trueba, J., 2018. Morphodynamics of barrier response to sea-level rise. In: Moore, L.J., Murray, A.B. (Eds.), Barrier Dynamics and Response to Climate Change. Springer International Publishing, Cham, Switzerland, pp. 277–304. http://dx.doi.org/10.1007/978-3-319-68086-6.
Barbier, E.B., Hacker, S.D., Kennedy, C., Koch, E.W., Stier, A.C., Silliman, B.R., 2011. The value of estuarine and coastal ecosystem services. Ecol. Monogr. 81, 169–193. http://dx.doi.org/10.1890/10-1510.1.
Belknap, D.F., Kraft, J.C., 1985. Influence of antecedent geology on stratigraphic preservation potential and evolution of Delaware's barrier systems. Mar. Geol. 63, 235–262. http://dx.doi.org/10.1016/0025-3227(85)90085-4.
Bernard, H.A., Major Jr., C.F., Parrott, B.S., 1959. The Galveston barrier island and environs: a model for predicting reservoir occurrence and trend. GCAGS Trans. 9, 221–224.
Billy, J., Robin, N., Hein, C.J., Certain, R., FitzGerald, D.M., 2015. Insight into the late Holocene sea-level changes in the NW Atlantic from a paraglacial beach-ridge plain south of Newfoundland. Geomorphology 248, 134–146. http://dx.doi.org/10.1016/j.geomorph.2015.07.033.
Blaauw, M., 2010. Methods and code for "classical" age-modelling of radiocarbon sequences. Quat. Geochronol. 5, 512–518. http://dx.doi.org/10.1016/j.quageo.2010.01.002.
Boon, J.D., Mitchell, M., 2015. Nonlinear change in sea level observed at North American tide stations. J. Coast. Res. 31 (6), 1295–1305. http://dx.doi.org/10.2112/JCOASTRES-D-15-00041.1.
Boon, J.D., Brubaker, J.M., Forrest, D.R., 2010. Chesapeake Bay land subsidence and sea level change: an evaluation of past and present trends and future outlook. In: Virginia Institute of Marine Science Special Report No. 425 in Applied Marine Science and Ocean Engineering, http://dx.doi.org/10.21220/V58X4P.
Bøtter-Jensen, L., Murray, A.S., 2001. Optically stimulated luminescence techniques in retrospective dosimetry. Radiat. Phys. Chem. 61, 181–190. http://dx.doi.org/10.1016/S0969-806X(01)00239-0.
Brander, L.M., Florax, R.J.G.M., Vermaat, J.E., 2006. The empirics of wetland valuation: a comprehensive summary and a meta-analysis of the literature. Environ. Resour. Econ. 33, 223–250. http://dx.doi.org/10.1007/s10640-005-3104-4.
Brenner, O.T., Moore, L.J., Murray, A.B., 2015. The complex influences of back-barrier deposition, substrate slope and underlying stratigraphy in barrier island response to sea-level rise: insights from the Virginia Barrier Islands, Mid-Atlantic Bight, U.S.A. Geomorphology 246, 334–350. http://dx.doi.org/10.1016/j.geomorph.2015.06.014.
Bristow, C.S., Pucillo, K., 2006. Quantifying rates of coastal progradation from sediment volume using GPR and OSL: the Holocene fill of Guichen Bay, south-east South Australia. Sedimentology 53, 769–788. http://dx.doi.org/10.1111/j.1365-3091.2006.00792.x.
Bronk Ramsey, C., 2009. Bayesian analysis of radiocarbon dates. Radiocarbon 51, 337–360. http://dx.doi.org/10.1017/S0033822200033865.
Carey, H.C., Lea, I., 1822. Geographical, Historical, And Statistical Map Of Virginia. Virginia. No. 22. Engraved by Young & Delleker. A Complet. Hist. Chronol. Geogr. Am. Atlas, Being A Guid. To Hist. North South Am. West Indies … To Year 1822. Accord. To Plan Le Sage's Atlas Intend. As A Companion To Lavoisne's Im.
Commonwealth of Virginia, 2007. Virginia Base Mapping Program.
Culver, S.J., Grand Pre, C.A., Mallinson, D.J., Riggs, S.R., Corbett, D.R., Foley, J., Hale, M., Metger, L., Ricardo, J., Rosenberger, J., Smith, C.G., Smith, C.W., Snyder, S.W., Twamley, D., Farrell, K.M., Horton, B.P., 2007. Late Holocene barrier island collapse. Sediment. Rec. 5, 4–8.
Davis, R.A., FitzGerald, D.M., 2004. Beaches and Coasts. Blackwell Publishing Ltd, Malden, MA.
Davis, R.A., Kuhn, B.J., 1985. Origin and development of Anclote Key, west-peninsular Florida. Mar. Geol. 63, 153–171. http://dx.doi.org/10.1016/0025-3227(85)90082-9.
Deaton, C.D., Hein, C.J., Kirwan, M.L., 2017. Barrier island migration dominates ecogeomorphic feedbacks and drives salt marsh loss along the Virginia Atlantic Coast, USA. Geology 45, 123–126. http://dx.doi.org/10.1130/G38459.1.
Demarest, J.M., Leatherman, S.P., 1985. Mainland influence on coastal transgression: Delmarva Peninsula. Mar. Geol. 63, 19–33. http://dx.doi.org/10.1016/0025-3227(85)90078-7.
Donnelly, J.P., Hawkes, A.D., Lane, P., Macdonald, D., Shuman, B.N., Toomey, M.R., Van Hengstum, P.J., Woodruff, J.D., 2015. Climate forcing of unprecedented intense-hurricane activity in the last 2000 years. Earth Futur. 3, 49–65. http://dx.doi.org/10.1002/2014EF000274.
Duc, A.W., Tye, R.S., 1987. Evolution and stratigraphy of a regressive barrier/backbarrier complex: Kiawah Island, South Carolina. Sedimentology 34, 237–251. http://dx.doi.org/10.1111/j.1365-3091.1987.tb00774.x.
Elias, E.P.L., Van Der Spek, A.J.F., 2006. Long-term morphodynamic evolution of Texel Inlet and its ebb-tidal delta (The Netherlands). Mar. Geol. 225, 5–21. http://dx.doi.org/10.1016/j.margeo.2005.09.008.
Engelhart, S.E., Horton, B.P., 2012. Holocene sea level database for the Atlantic coast of the United States. Quat. Sci. Rev. 54, 12–25. http://dx.doi.org/10.1016/j.quascirev.2011.09.013.
Engelhart, S.E., Horton, B.P., Douglas, B.C., Peltier, W.R., Törnqvist, T.E., 2009. Spatial variability of late Holocene and 20th century sea-level rise along the Atlantic coast of the United States. Geology 37, 1115–1118. http://dx.doi.org/10.1130/G30360A.1.
Fallon, A.R., Hein, C.J., Rosen, P.S., Gannon, H.L., 2015. Cyclical shoreline erosion: the impact of a jettied river mouth on the downdrift barrier island. In: Coastal Sediments '15, Proceedings of the 11th International Symposium on Coastal Engineering and Science of Coastal Sediment Processes.
Fenster, M., Dolan, R., 1996. Assessing the impact of tidal inlets on adjacent barrier island shorelines. J. Coast. Res. 12, 294–310. http://dx.doi.org/10.2112/JCOASTRES-D-12-00.
Fenster, M.S., McBride, R.A., 2015. Barrier-island geology and morphodynamics along the open-ocean coast of the Delmarva Peninsula: an overview. In: McBride, R.A., Fenster, M.S., Seminack, C.T., Richardson, T.M., Sepanik, J.M., Hanley, J.T., Bundick, J.A., Tedder, E. (Eds.), Holocene Barrier-Island Geology and Morphodynamics of the Maryland and Virginia Open-Ocean Coasts: Fenwick, Assateague, Chincoteague, Wallops, Cedar, and Parramore Islands, in: Brezinski, D.K., Halka, J.P., and Ortt, R.A. (Eds.), Tripping from the Fall Line: Field Excursions for the GSA Annual Meeting, Baltimore, 2015: Geological Society of America Field Guide. 40. pp. 310–334.
Fenster, M.S., Dolan, R., Smith, J.J., 2016. Grain-size distributions and coastal

morphodynamics along the southern Maryland and Virginia barrier islands. Sedimentology 63, 809–823. http://dx.doi.org/10.1111/sed.12239.
Fenster, M.S., Rizzo, B., McManus, J., 2017. Non-linear shoreline change modeling of the northern Virginia coast: Virginia Barrier Islands and Assateague Island. In: Southeastern Section of the Geological Society of America. Richmond, VA, http://dx.doi.org/10.1130/abs/2017SE-291183.
Finkelstein, K., Ferland, M.A., 1987. Back-barrier response to sea-level rise, Eastern Shore of Virginia. In: Nummedal, D., Pilkey, O.H., Howard, J. (Eds.), Sea-Level Fluctuations and Coastal Evolution. SEPM (Society for Sedimentary Geology)pp. 145–155. http://dx.doi.org/10.2110/pec.87.41.0145.
Finkelstein, K., Kearney, M.S., 1988. Late Pleistocene barrier-island sequence along the southern Delmarva Peninsula: implications for middle Wisconsin sea levels. Geology 16, 41–45.
FitzGerald, D.M., 1984. Interactions between the ebb-tidal delta and landward shoreline: Price Inlet, South Carolina. J. Sediment. Res. 54, 1303–1318. http://dx.doi.org/10.1306/212F85C6-2B24-11D7-8648000102C1865D.
FitzGerald, D.M., 1988. Shoreline erosional-depositional processes associated with tidal inlets. In: Aubrey, D.G., Weishar, L. (Eds.), Hydrodynamics and Sediment Dynamics of Tidal Inlets. Springer New York, New York, NY, pp. 186–225. http://dx.doi.org/10.1029/LN029p0186.
FitzGerald, D.M., Penland, S., Nummedal, D., 1984. Control of barrier island shape by inlet sediment bypassing: East Frisian Islands, West Germany. Mar. Geol. 60, 355–376. http://dx.doi.org/10.1016/0025-3227(84)90157-9.
FitzGerald, D.M., Buynevich, I.V., Rosen, P.S., 2001. Geological evidence of former tidal inlets along a retrograding barrier Duxbury Beach. J. Coast. Res. SI 34, 1–13.
FitzGerald, D.M., Fenster, M.S., Argow, B.A., Buynevich, I.V., 2008. Coastal impacts due to sea-level rise. Annu. Rev. Earth Planet. Sci. 36, 601–647. http://dx.doi.org/10.1146/annurev.earth.35.031306.140139.
FitzGerald, D.M., Hein, C.J., Hughes, Z., Kulp, M., Georgiou, I., Miner, M., 2018. Runaway barrier island transgression concept: Global case studies. In: Moore, L.J., Murray, A.B. (Eds.), Barrier Dynamics and Response to Climate Change. Springer International Publishing, Cham, Switzerland, pp. 3–56. http://dx.doi.org/10.1007/978-3-319-68086-6_1.
Foyle, A.M., Oertel, G.F., 1997. Transgressive systems tract development and incised-valley fills within a Quaternary estuary-shelf system: Virginia inner shelf, USA. Mar. Geol. 137, 227–249. http://dx.doi.org/10.1016/S0025-3227(96)00092-8.
Fruergaard, M., Møller, I., Johannessen, P.N., Nielsen, L.H., Andersen, T.J., Nielsen, L., Sander, L., Pejrup, M., 2015. Stratigraphy, evolution, and controls of a Holocene transgressive – regressive barrier island under changing sea level: Danish North Sea coast. J. Sediment. Res. 85, 820–844. http://dx.doi.org/10.2110/jsr.2015.53.
FSA, 1967. Photo Number: AR1SWBA00020058.
Goldstein, E.B., Moore, L.J., Durán Vinent, O., 2017. Lateral vegetation growth rates exert control on coastal foredune hummockiness and coalescing time. Earth Surf. Dyn. 5, 417–427. http://dx.doi.org/10.5194/esurf-5-417-2017.
Halsey, S., 1978. Late Quaternary Geologic History and Morphologic Development of the Barrier Island System Along the Delmarva Peninsula of the Mid-Atlantic Bight (PhD Thesis). University of Delaware.
Harris, M.S., 1992. The Geomorphology of Hog Island, Virginia: A Mid-Atlantic Coast Barrier (M.S. Thesis). University of Virginia.
Harrison, W., Malloy, R.J., Rusnak, G.A., Terasmae, J., 1965. Possible Late Pleistocene uplift: Chesapeake Bay entrance. J. Geol. 73, 201–229. http://dx.doi.org/10.1086/jg.73.2.30080961.
Hayden, B.P., 2003. Annual Number of Storms on the Virginia Coast 1885–2002. http://dx.doi.org/10.6073/pasta/82e73bf8b54f5888fa9488ff3af7aa4f.
Hayden, B.P., Hayden, N.R., 2003. Decadal and century-long changes in storminess at long-term ecological research sites. In: Greenland, D., Goodin, D.G., Smith, R.S. (Eds.), Climate Variability and Ecosystem Response at Long-Term Ecological Research Sites. Oxford University Press, New York, pp. 262–285.
Hayden, B.P., Santos, M.C.F.V., Shao, G., Kochel, R.C., 1995. Geomorphological controls on coastal vegetation at the Virginia Coast Reserve. Geomorphology 13, 283–300. http://dx.doi.org/10.1016/0169-555X(95)00032-Z.
Hayes, M.O., 1979. Barrier island morphology as a function of tidal and wave regime. In: Leatherman, S.P. (Ed.), Barrier Islands: From the Gulf of St. Lawrence to the Gulf of Mexico. Academic Press, New York, pp. 1–27.
Hayes, M.O., 1994. The Georgia Bight barrier system. In: Davis, R.A. (Ed.), Geology of Holocene Barrier Island Systems. Springer, pp. 233–304. http://dx.doi.org/10.1007/978-3-642-78360-9.
Hein, C.J., FitzGerald, D.M., Carruthers, E.A., Stone, B.D., Barnhardt, W.A., Gontz, A.M., 2012. Refining the model of barrier island formation along a paraglacial coast in the Gulf of Maine. Mar. Geol. 307–310, 40–57. http://dx.doi.org/10.1016/j.margeo.2012.03.001.
Hein, C.J., FitzGerald, D.M., de Menezes, J.T., Cleary, W.J., Klein, A.H.F., Albernaz, M.B., 2014. Coastal response to late-stage transgression and sea-level highstand. Bull. Geol. Soc. Am. 126, 459–480. http://dx.doi.org/10.1130/B30836.1.
Kemp, A.C., Horton, B.P., Donnelly, J.P., Mann, M.E., Vermeer, M., Rahmstorf, S., 2011. Climate related sea-level variations over the past two millennia. Proc. Natl. Acad. Sci. 108, 11017–11022. http://dx.doi.org/10.1073/pnas.1015619108.
Kochel, R.C., Kahn, J.H., Dolan, R., Hayden, B.P., May, P.F., 1985. U.S. Mid-Atlantic barrier island geomorphology. J. Coast. Res. 1, 1–9.
Krantz, D.E., Hobbs III, C.H., Wikel, G.L., 2016. Atlantic coast and inner shelf. In: Bailey, C.M., Sherwood, W.C., Eaton, L.S., Powards, D.S. (Eds.), Geology of Virginia. Virginia Museum of Natural History, pp. 341–380.
Lazar, K.B., Mallinson, D.J., Culver, S.J., 2016. Late Quaternary development of the Croatan Beach Ridge Complex, Bogue Sound, Bogue Banks, NC, USA and implications for coastal evolution. Estuar. Coast. Shelf Sci. 174, 49–64. http://dx.doi.org/10.1016/j.ecss.2016.03.016.
Leatherman, S.P., Rice, T.E., Goldsmith, V., 1982. Virginia Barrier Island configuration: a reappraisal. Science 215, 285–287. http://dx.doi.org/10.1007/s13398-014-0173-7.2.
Lorenzo-Trueba, J., Ashton, A.D., 2014. Rollover, drowning, and discontinuous retreat: distinct modes of barrier response to sea-level rise arising from a simple morphodynamic model. J. Geophys. Res. Earth Surf. 119, 779–801. http://dx.doi.org/10.1002/2013JF002941.
Lorenzo-Trueba, J., Mariotti, G., 2017. Chasing boundaries and cascade effects in a coupled barrier-marsh-lagoon system. Geomorphology 290, 153–163. http://dx.doi.org/10.1016/j.geomorph.2017.04.019.
Mallinson, D.J., Burdette, K., Mahan, S., Brook, G., 2008. Optically stimulated luminescence age controls on late Pleistocene and Holocene coastal lithosomes, North Carolina, USA. Quat. Res. 69, 97–109. http://dx.doi.org/10.1016/j.yqres.2007.10.002.
Mallinson, D.J., Smith, C.W., Mahan, S., Culver, S.J., McDowell, K., 2011. Barrier island response to late Holocene climate events, North Carolina, USA. Quat. Res. 76, 46–57. http://dx.doi.org/10.1016/j.yqres.2011.05.001.
Mallinson, D.J., Culver, S.J., Leorri, E., Mitra, S., Mulligan, R., Riggs, S.R., 2018. Barrier island and estuary co-evolution in response to Holocene climate and sea-level change: Pamlico Sound and the Outer Banks barrier islands, North Carolina, USA. In: Moore, L.J., Murray, A.B. (Eds.), Barrier Dynamics and Response to Changing Climate. Springer International Publishing, Cham, Switzerland, pp. 91–210. http://dx.doi.org/10.1007/978-3-319-68086-6.
Markey, B.G., Bøtter-Jensen, L., Duller, G.A.T., 1997. A new flexible system for measuring thermally and optically stimulated luminescence. Radiat. Meas. 27, 83–89. http://dx.doi.org/10.1016/S1350-4487(96)00126-6.
McBride, R.A., Richardson, T.M., Fenster, M.S., Seminack, C.T., 2015. Shoreline and ecogeomorphic changes along Parramore Island, Virginia: a mixed-energy, tide-dominated barrier island. In: McBride, R.A., Fenster, M.S., Seminack, C.T., Richardson, T.M., Sepanik, J.M., Hanley, J.T., Bundick, J.A., Tedder, E. (Eds.), Holocene Barrier-Island Geology and Morphodynamics of the Maryland and Virginia Open-Ocean Coasts: Fenwick, Assateague, Chincoteague, Wallops, Cedar, and Parramore Islands, in: Brezinski, D.K., Halka, J.P., and Ortt, R.A. (Eds.), Tripping from the Fall Line: Field Excursions for the GSA Annual Meeting, Baltimore, 2015: Geological Society of America Field Guide. 40. pp. 370–384.
McMillan, B.A., Day, F.P., 2010. Micro-environment and plant assemblage structure on Virginia's Barrier Island "pimple" dunes. Northeast. Nat. 17, 473–492.
Missimer, T., 1973. Growth rate of beach ridges on Sanibel Island. FL. Trans. Gulf Coast Assoc. Geol. Soc. 23, 383–388.
Moore, L.J., List, J.H., Williams, S.J., Stolper, D., 2010. Complexities in barrier island response to sea level rise: insights from numerical model experiments, North Carolina Outer Banks. J. Geophys. Res. 115, F03004. http://dx.doi.org/10.1029/2009JF001299.
Moran, K.L., Mallinson, D.J., Culver, S.J., Leorri, E., Mulligan, R.P., 2015. Late Holocene evolution of Currituck Sound, North Carolina, USA: environmental change driven by sea-level rise, storms, and barrier island morphology. J. Coast. Res. 31 (4), 827–841. http://dx.doi.org/10.2112/JCOASTRES-D-14-00069.1.
Morton, R.A., 1994. Texas barriers. In: Davis, R.A. (Ed.), Geology of Holocene Barrier Island Systems. Springer, pp. 75–114.
Morton, R.A., Donaldson, A.C., 1973. Sediment distribution and evolution of tidal deltas along a tide-dominated shoreline, Wachapreague, Virginia. Sediment. Geol. 10, 285–299. http://dx.doi.org/10.1016/0037-0738(73)90053-5.
Morton, R.A., Price, W.A., 1987. Late Quaternary sea-level fluctuations and sedimentary phases of the Texas coastal plain and shelf. In: Nummedal, D., Pilkey, O.H., Howard, J.D. (Eds.), Sea-Level Fluctuations and Coastal Evolution. SEPM (Society for Sedimentary Geology)pp. 181–198.
Moslow, T.F., 1980. Stratigraphy of Mesotidal Barrier Islands (PhD Thesis). University of South Carolina.
Moslow, T.F., Heron, S.D., 1978. Relict inlets; preservation and occurrence in the Holocene stratigraphy of southern core banks, North Carolina. J. Sediment. Res. 48, 1275–1286. http://dx.doi.org/10.1306/212f765d-2b24-11d7-8648000102c1865d.
Moslow, T.F., Tye, R.S., 1985. Recognition and characterization of Holocene tidal inlet sequences. Mar. Geol. 63, 129–151. http://dx.doi.org/10.1016/0025-3227(85)90081-7.
Munsell, 2000. Munsell Soil Color Charts. GretagMacbeth, New Windsor.
Murray, A.S., Wintle, A.G., 2000. Luminescence dating of quartz using an improved single-aliquot regenerative-dose protocol. Radiat. Meas. 32, 57–73. http://dx.doi.org/10.1016/S1350-4487(99)00253-X.
Newman, W.S., Munsart, C.A., 1968. Holocene geology of the Wachapreague lagoon, Eastern Shore Peninsula, Virginia. Mar. Geol. 6, 81–105. http://dx.doi.org/10.1016/0025-3227(68)90014-5.
Newman, W.S., Rusnak, G.A., 1965. Holocene submergence of the Eastern Shore of Virginia. Science 148, 1464–1466. http://dx.doi.org/10.1126/science.148.3676.1464.
Nooren, K., Hoek, W., Winkels, T., Huizinga, A., Van Der Plicht, H., Van Dam, R.L., Van Heteren, S., Van Bergen, M.J., Prins, M.A., Reimann, T., Wallinga, J., Cohen, K.M., Minderhoud, P., Middelkoop, H., 2017. The Usumacinta-Grijalva beach-ridge plain in southern Mexico: a high-resolution archive of river discharge and precipitation. Earth Surf. Dyn. 5, 529–556. http://dx.doi.org/10.5194/esurf-5-529-2017.
Oertel, G.F., 1979. Barrier island development during the Holocene recession, southeastern United States. In: Leatherman, S.P. (Ed.), Barrier Islands: From the Gulf of St. Lawrence to the Gulf of Mexico. Academic Press, New York, pp. 273–290.
Oertel, G.F., Foyle, A.M., 1995. Drainage displacement by sea-level fluctuation at the outer margin of the Chesapeake Seaway. J. Coast. Res. 11, 583–604.
Oertel, G.F., Overman, K., 2004. Sequence morphodynamics at an emergent barrier island, Middle Atlantic coast of North America. Geomorphology 58, 67–83. http://dx.

doi.org/10.1016/S0169-555X(03)00187-9.
Oertel, G.F., Kearney, M.S., Leatherman, S.P., Woo, H., 1989. Anatomy of a barrier platform: outer barrier lagoon, southern Delmarva Peninsula, Virginia. Mar. Geol. 88, 303–318. http://dx.doi.org/10.1016/0025-3227(89)90103-5.
Oertel, G.F., Kraft, J.C., Kearney, M.S., Woo, H.J., 1992. A rational theory for barrier-lagoon development. In: Fletcher, C.H., Wehmiller, J.F. (Eds.), Quaternary Coasts of the United States: Marine and Lacustrine Systems. SEPM (Society for Sedimentary Geology)pp. 77–87. http://dx.doi.org/10.2110/pec.92.48.0077.
Otvos, E.G., 2012. Coastal barriers - nomenclature, processes, and classification issues. Geomorphology 139–140, 39–52. http://dx.doi.org/10.1016/j.geomorph.2011.10.037.
Park, J.-Y., Wells, J.T., 2007. Spit growth and downdrift erosion: results of longshore transport modeling and morphologic analysis at the cape lookout cuspate foreland. J. Coast. Res. 23, 553–568. http://dx.doi.org/10.2112/03-0116.1.
Psuty, N.P., 2008. The coastal foredune: a morphological basis for regional coastal dune development. In: Martinez, M.L., Psuty, N.P. (Eds.), Coastal Dunes: Ecology and Conservation (Ecological Studies). Springer, Berlin, Heidelberg, pp. 11–27. http://dx.doi.org/10.1007/978-3-540-74002-5_2.
Reimer, P.J., Bard, E., Bayliss, A., Beck, J.W., Blackwell, P.G., Ramsey, C.B., Buck, C.E., Cheng, H., Edwards, R.L., Friedrich, M., Grootes, P.M., Guilderson, T.P., Haflidason, H., Hajdas, I., Hatté, C., Heaton, T.J., Hoffmann, D.L., Hogg, A.G., Hughen, K.A., Kaiser, K.F., Kromer, B., Manning, S.W., Niu, M., Reimer, R.W., Richards, D.A., Scott, E.M., Southon, J.R., Staff, R.A., Turney, C.S.M., van der Plicht, J., 2013. IntCal13 and Marine13 radiocarbon age calibration curves 0–50,000 years cal BP. Radiocarbon 55, 1869–1887. http://dx.doi.org/10.2458/azu_js_rc.55.16947.
Rice, T.E., Niedoroda, A.W., Pratt, A.P., 1976. The coastal processes and geology: Virginia barrier islands. In: Ecosystem Description: The Virginia Coast Reserve Study, pp. 107–384.
Richardson, T.M., 2012. Morphodynamic Changes of the Parramore-Cedar Barrier-island System and Wachapreague Inlet, Virginia From 1852 to 2011: A Model of Barrier Island and Tidal Inlet Evolution Along the Southern Delmarva Peninsula, USA (PhD Thesis). George Mason University.
Rick, T.C., Henkes, G.A., Lowery, D.L., Colman, S.M., Culleton, B.J., 2012. Marine radiocarbon reservoir corrections (ΔR) for Chesapeake Bay and the Middle Atlantic Coast of North America. Quat. Res. 77, 205–210. http://dx.doi.org/10.1016/j.yqres.2011.11.002.
Riggs, S.R., Cleary, W.J., Snyder, S.W., 1995. Influence of inherited geologic framework on barrier shoreface morphology and dynamics. Mar. Geol. 126, 213–234. http://dx.doi.org/10.1016/0025-3227(95)00079-E.
Rink, W.J., López, G.I., 2010. OSL-based lateral progradation and aeolian sediment accumulation rates for the Apalachicola Barrier Island Complex, North Gulf of Mexico, Florida. Geomorphology 123, 330–342. http://dx.doi.org/10.1016/j.geomorph.2010.08.001.
Rodriguez, A.B., Anderson, J.B., Siringan, F.P., Taviani, M., 2004. Holocene evolution of the east Texas coast and inner continental shelf: along-strike variability in coastal retreat rates. J. Sediment. Res. 74, 405–421. http://dx.doi.org/10.1306/092403740405.
Rogers, L.J., Moore, L.J., Goldstein, E.B., Hein, C.J., Lorenzo-Trueba, J., Ashton, A.D., 2015. Anthropogenic controls on overwash deposition: evidence and consequences. J. Geophys. Res. Earth Surf. 120, 2609–2624. http://dx.doi.org/10.1002/2015JF003634.
Rusnak, G.A., Bowman, A.L., Östlund, H.G., 1963. Miami natural radiocarbon measurements II. Radiocarbon 5, 23–33. http://dx.doi.org/10.1017/S0033822200036754.
Ruz, M.-H., Héquette, A., Marin, D., Sipka, V., Crapoulet, A., Cartier, A., 2017. Development of an incipient foredune field along a prograding macrotidal shoreline, northern France. Géomorphol. Reli. Process. Environ. 23, 37–50. http://dx.doi.org/10.4000/geomorphologie.11638.
Seminack, C.T., Buynevich, I.V., 2013. Sedimentological and geophysical signatures of a relict tidal inlet complex along a wave-dominated barrier: Assateague Island, Maryland, U.S.A. J. Sediment. Res. 83, 132–144. http://dx.doi.org/10.2110/jsr.2013.10.
Seminack, C.T., McBride, R.A., 2015. Geomorphic history and diagnostic features of former tidal inlets along Assateague Island, Maryland-Virginia: a life-cycle model for inlets along wave-dominated barrier islands. Shore & Beach 83, 3–24.
Stallins, J.A., Corenblit, D., 2017. Interdependence of geomorphic and ecologic resilience properties in a geographic context. Geomorphology 305, 76–93. http://dx.doi.org/10.1016/j.geomorph.2017.09.012.
Stutz, M.L., Pilkey, O.H., 2011. Open-ocean barrier islands: global influence of climatic, oceanographic, and depositional settings. J. Coast. Res. 27 (2), 207–222. http://dx.doi.org/10.2112/09-1190.1.
Timmons, E.A., Rodriguez, A.B., Mattheus, C.R., DeWitt, R., 2010. Transition of a regressive to a transgressive barrier island due to back-barrier erosion, increased storminess, and low sediment supply: Bogue Banks, North Carolina, USA. Mar. Geol. 278, 100–114. http://dx.doi.org/10.1016/j.margeo.2010.09.006.
Tye, R.S., Moslow, T.F., 1993. Tidal inlet reservoirs: insights from modern examples. In: Rhodes, E.G., Moslow, T.F. (Eds.), Marine Clastic Reservoirs: Examples and Analogues. Springer New York, New York, NY, pp. 77–99. http://dx.doi.org/10.1007/978-1-4757-0160-9_4.
US Coast and Geodetic Survey, 1933. Chincoteague Inlet to Hog Island Light.
US Coast Survey, 1855. Preliminary Chart of Part of the Sea Coast of Virginia and Entrance to Chesapeake Bay With Entrance to Chesapeake Bay.
USGS, 2016. Topobathymetric Model for Chesapeake Bay Region - District of Columbia, States of Delaware, Maryland, Pennsylvania, and Virginia, 1859 to 2015, 1st ed. .
Van de Plassche, O., 1990. Mid-Holocene sea-level change on the Eastern Shore of Virginia. Mar. Geol. 91, 149–154. http://dx.doi.org/10.1016/0025-3227(90)90138-A.
Walters, D., Moore, L.J., Duran Vinent, O., Fagherazzi, S., Mariotti, G., 2014. Interactions between barrier islands and backbarrier marshes affect island system response to sea level rise: insights from a coupled model. J. Geophys. Res. Earth Surf. 119, 2013–2031. http://dx.doi.org/10.1002/2014JF003091.
Wikel, G.L., 2008. Variability in Geologic Framework and Shoreline Chang: Assateague and Wallops Islands, Eastern Shore of Virginia (M.S. Thesis). Virginia Institute of Marine Science.
Wolinsky, M.A., Murray, A.B., 2009. A unifying framework for shoreline migration: 2. Application to wave-dominated coasts. J. Geophys. Res. 114, F01009. http://dx.doi.org/10.1029/2007JF000856.
Wright, E., Kruse, S., Forman, S.L., Harris, M.S., 2018. Millennial scale development of a southeastern United States spit. J. Coast. Res. 34, 255–271. http://dx.doi.org/10.2112/JCOASTRES-D-16-00005.1.
Zaremba, N., Mallinson, D.J., Leorri, E., Culver, S., Riggs, S., Mulligan, R., Horsman, E., Mitra, S., 2016. Controls on the stratigraphic framework and paleoenvironmental change within a Holocene estuarine system: Pamlico Sound, North Carolina, USA. Mar. Geol. 379, 109–123. http://dx.doi.org/10.1016/j.margeo.2016.04.012.